

Dear Dr. Blume and reviewers:

Thank you very much for your comments on our manuscript. We have made correction or given explanations in response to your comments. Please see below our responses in blue to all your comments. The marked-up version is also attached following the responses to the comments.

Sincerely,

Wei Hu

Bing Cheng Si

.....

Interactive comment on “Estimating spatially distributed soil water content at small watershed scales based on decomposition of temporal anomaly and time stability analysis” by W. Hu and

B. C. Si

Anonymous Referee #1

Received and published: 4 August 2015

Manuscript hessd-12-6467-2015 introduces an empirical orthogonal function (EOF) approach for analysing spatio-temporal patterns in soil water content observations. The presented approach is similar to other principal component analyses recently applied to spatio-temporally resolved geo-data. The approach may be seen as an extension to the one presented by Parry and Niemann (2007), a reference that is frequently cited in the manuscript. Parry and Niemann (2007) first extract the spatial arithmetic average soil water content from the 2-D spatio-temporally resolved measurement data. They then apply an EOF on the residuals which are consequently split into expansion coefficients (ECs, i.e. the eigenvectors of the space-time matrix of residuals) and empirical orthogonal functions (EOFs, i.e. the residuals mapped on the eigenvectors). EOFs may then be used to identify regions with similar hydrologic behaviour or to down-scale average water contents of the entire region. The novelty of the approach presented in hessd-12-6467-2015 is that first the temporal arithmetic average is subtracted from the data as in Mittelbach and Seneviratne (2012, also frequently cited). In a next step, the spatially constant fraction is isolated from the residuals. The EOF is then only applied on the residuals of the residuals. The authors discuss cases in which their approach has advantages over the one of Perry and Niemann (2007) and demonstrate that their approach yields water content better cross-correlation results for a dataset collected long a transect in the Canadian prairies.

The manuscript hessd-12-6467-2015 is in an already well developed state which made it relatively easy to read. As far as I can judge the English is good with only a few exception missing articles and occasional strange wording. The manuscript is largely well-structured albeit

that I think that the manuscript would gain if the discussion on when the here presented EOF approach is advantageous (P6484,L12 – P6485,L23) was moved to the material and method section. As the authors write on P6484,L16 and L23, most of the text in these three paragraphs is founded on theory and is known a priori. I think it would make it easier to understand the new approach if the circumstances under which it is advantageous would already be quantitatively explained in the material and methods section. Moreover, the discussion section could be improved by better separating discussions i) on correlations between site factors and time events with model parameters (e.g. M_{tn} or EOF1) and ii) on prediction performance of the model. Also, the conclusions are more of a summary in its present state.

Response:

Thank you for reviewing our manuscript and your positive and constructive comments. Please refer to all changes in the revised manuscript following our response.

(1) We have checked the English carefully again, and we also had a colleague checked the language. The required articles were added.

(2) We moved the discussion on situations that the TA model is advantageous in theory into the material and method on Lines 286-309 immediately after introducing the NSCE to evaluate the quality of estimation of spatially distributed SWC. We believe the following three aspects affect the relative performance of the TA model over the SA model: the amount of R_{tn} variance considered in the TA model, the degree of non-linearity between the $M_{\hat{tn}}$ and EOF1 of the R_{tn} , and the estimation accuracy of the EC_t from the cosine function (Eq.4).

Therefore, we changed it as "**Many factors may affect the relative performance of spatially distributed SWC estimation between the TA model and the SA model. First, the degree of outperformance of the TA model over the SA model may depend on the amount of R_{tn} variance considered in the TA model. On one hand, the two models are identical if variance of R_{tn} is close to zero or there are negligible interactions between the spatial and temporal components (Fig. 1). On the other hand, if no underlying spatial patterns exist in the R_{tn} or the underlying spatial patterns contributed little to the total variance of the R_{tn} , the outperformance will also be very limited. Therefore, the greater the variance of R_{tn} considered in the TA model, the more likely the TA model can outperform the SA model.**

Second, the way of EOF decomposition may also affect the relative performance. In the SA model, EOF decomposition is performed on lumped time-stable patterns ($M_{\hat{m}}$) and space-variant temporal anomaly (R_m). In the TA model, however, EOF decomposition is made only on the R_m . In theory, the two models will be identical if the $M_{\hat{m}}$ and the first underlying spatial pattern (i.e., EOF1) of the R_m were perfectly correlated. If a nonlinear relationship exists between them, lumping the $M_{\hat{m}}$ and R_m together, as in the SA model, would weaken the model performance as compared to the TA model. From this aspect, the greater deviation from a linear relationship between the $M_{\hat{m}}$ and EOF1 of the R_m , may lead to a greater outperformance of the TA model over the SA model. Finally, the performances of both models rely on the estimation accuracy of the EC_t which depends on both goodness of fit of the cosine function (i.e., Eq. 4) and estimation accuracy of the $S_{\hat{m}}$. Because the same $S_{\hat{m}}$ values are used for the two models, the relative performance of the two models is related to the goodness of fit of Eq. (4)."

Meanwhile, we also discussed the three factors that can influence the model performance by considering the real situation of our datasets, which can deepen our understanding of the model performance. We put this discussion in to "4.2 Model performance for spatially distributed SWC estimation" (Line 537-610). We changed this part as:

" 4.2 Model performance for spatially distributed SWC estimation

The outperformance of the TA model for estimating spatial SWC at the Canadian site and Chinese site can be partly explained by the high contribution percentages (average of 19–118%) of the $\sigma_{\hat{m}}^2(R_m)$ to the total variance. When SWC is close to average levels, R_m is also close to zero, resulting in negligible variance contribution from R_m to the total variance. In this case, the soil water patterns are stable, the SA model performs well, and there will be little differences between these two models. As is well known, the spatial patterns in soil water content are inherently time unstable. For example, when evapotranspiration becomes the dominant process at the small watershed scale, more water

will be lost in depressions due to the denser vegetation than on knolls (Millar, 1971; Biswas et al., 2012), effectively diminishing the spatial patterns and increasing temporal instability. In this case, the $\sigma_{\hat{n}}^2(R_m)$ contributes more to the total variance (e.g., high up to 632%) and the TA model may outperform the SA model. This explained why the outperformance of the TA model was more obvious in the dry conditions. For the GENCAI network in Italy, although the $\sigma_{\hat{n}}^2(R_m)$ contributed 68% of the total variance, the performance of the TA model was identical to the SA model. This was because there were no underlying spatial patterns in the R_m . Similarly, because the first underlying spatial pattern (i.e., EOF1) explained greater percentages of the $\sigma_{\hat{n}}^2(R_m)$ at the Canadian site (44–61%) than the Chinese site (23%), the outperformance of the TA model over the SA model was more obvious at the former site (Fig. 9 and 10a). Therefore, the TA model is advantageous only if the contribution of $\sigma_{\hat{n}}^2(R_m)$ to the total variance is substantial and underlying spatial patterns exist in the R_m .

The existence of underlying spatial patterns in the R_m is related to the controlling factors, which may be scale-specific. At small scales, “static” factors such as the depth to the CaCO₃ layer and SOC at the Canadian site may affect not only the time-stable patterns but also the R_m . The persistent influence of “static” factors on the R_m resulted in significant underlying spatial patterns in the R_m . Thus, the TA model outperformed the SA model at the small scales. At large scales such as the basin scale or greater, time-stable patterns may be controlled by, in addition to soil and topography (Mittelbach and Seneviratne, 2012), the climate gradient (Sherratt and Wheater, 1984); at those scales, R_m

is more likely to be controlled by the meteorological anomaly (i.e., spatially random variation) (Walsh and Mostek, 1980), and the effects of soil and topography may be reduced. Consequently, spatial patterns in the R_{tn} may be weakened and the TA model may have no advantages over the SA model such as for the Italian site.

The $M_{\hat{in}}$ and the underlying spatial patterns (EOF1) in the R_{tn} were controlled by the same spatial forcing (e.g., depth to CaCO₃ layer and SOC) at the Canadian site (Table 1), and they were correlated with an R^2 of 0.83 for the near surface and 0.42 for the root zone. Although the relationships between $M_{\hat{in}}$ and R_{tn} were strong, they were not strictly linear, suggesting that $M_{\hat{in}}$ and R_{tn} were affected differently by these factors. Therefore, the nonlinear relationship between $M_{\hat{in}}$ and R_{tn} partially contributed to the outperformance of the TA model over the SA model.

The relationship between the $S_{\hat{in}}$ and EC1 was better fitted by the cosine function in the TA model than the SA model (Figs. 4b and 6b), with R^2 of 0.76 versus 0.73 in the near surface and 0.88 versus 0.73 in the root zone. The reduced scatter in the $S_{\hat{in}}$ and EC1 relationship for the TA model may also partly explain the outperformance of the TA model over the SA model.

Therefore, the outperformance of the TA model over the SA model depends on counterbalance among the variance of R_{tn} explained in the TA model, the linear correlation between the $M_{\hat{in}}$ and EOF1 of the R_{tn} , and the goodness of fit for the $S_{\hat{in}}$ and EC1 relationship. For example, the variance of EOF1 in the R_{tn} for the near surface (i.e.,

264%²) was much greater than that for the root zone (i.e., 43%²). However, $M_{\hat{m}}$ and underlying spatial patterns (EOF1) in the R_{tn} in the root zone deviated more from a linear relationship, and the reduced scatter in the $S_{\hat{m}}$ and EC1 relationship in the TA model was more obviously in the root zone than in the near surface. As a result, the outperformance of the TA model was comparable between the near surface and root zone at the Canadian site (Fig. 9).

In the real world, the relations between the $M_{\hat{m}}$ and underlying spatial patterns in the R_{tn} may rarely be perfectly linear. Therefore, when underlying spatial patterns exist in the R_{tn} and the R_{tn} has substantial variances, the TA model is preferable to the SA model for the estimation of spatially distributed SWC. Because the TA model was not worse than the SA model for the whole range of SWC, the TA model is suggested for the estimation of spatially distributed SWC at different soil water conditions.

Previous studies on SWC decomposition mainly focus on near surface layers (Jawson and Niemann, 2007; Perry and Niemann, 2007, 2008; Joshi and Mohanty, 2010; Korres et al., 2010; Busch et al., 2012). This study decomposed spatiotemporal SWC using the TA model for both the near surface and the root zone. The results showed that the estimation of spatially distributed SWC at small watershed scales was improved by the TA method that considers the R_{tn} . Because of the stronger time stability of SWC in deeper soil layers (Biswas and Si, 2011), SWC evaluation in thicker soil layers was more accurate than in shallow soil layers. This is particularly important because SWC data for deeper soil layers in a watershed is more difficult to collect than that of surface soil."

(3) We separated the discussion into two parts:

4.1 Controls of the $M_{\hat{m}}$ and R_{tn}

4.2 Model performance for spatially distributed SWC estimation

(4) We changed the conclusions to make it more concise. Meanwhile, the future study and the possible limitation of this method were also added (Lines 612-642). Therefore, we changed it as:

" The TA model was used to decompose spatiotemporal SWC into time-stable patterns $M_{\hat{m}}$, space-invariant temporal anomaly $A_{\hat{m}}$, and space-variant temporal anomaly R_{tn} . This study indicated that underlying spatial patterns may exist in the R_{tn} at small scales (e.g., small watersheds and hillslope) but may not exist at large scales such as the GENCAI network (~250 km²) in Italy. This was because the R_{tn} at small scales was driven by “static” factors such as depth to the CaCO₃ layer and SOC at the Canadian site, while the R_{tn} at large scales may be dominated by “dynamic” factors such as meteorological anomaly. Compared to the SA model, estimation of spatially distributed SWC was improved with the TA model at small watershed scales. This was because the TA model considered a fair amount of spatial variance in the R_{tn} , which was ignored in the SA model. Furthermore, the improved performance was observed mainly when there was less or more soil water than the average level, especially in drier conditions due to the high $\sigma_{\hat{n}}^2(R_{tn})$ value.

This study showed that outperformance of the TA model over the SA model is possible when $\sigma_{\hat{n}}^2(R_{tn})$ contributes substantial variance to the total variance of SWC, and significant spatial patterns (or EOFs) exist in the R_{tn} . Further application of the TA model for the estimation of spatially distributed SWC at different scales and hydrological backgrounds is recommended. If the TA model parameters (i.e., $M_{\hat{m}}$, EOF1 of the R_{tn} , and relationship between EC and $S_{\hat{m}}$) are obtained from historical SWC datasets, a detailed

spatially distributed SWC of near surface soil at watershed scales can be constructed from remote sensed SWC. Note that both models rely on previous SWC measurements for model parameters. Therefore, the future study should be directed to estimate spatially distributed SWC in un-gauged watersheds based on the estimation of the model parameters using pedotransfer functions. Since the TA model needs one more spatial parameter (i.e., $M_{\hat{t}n}$) than the SA model, the advantage of the TA model may be weakened. Nevertheless, the TA model may be preferred if it estimates spatial SWC much better than the SA model such as under dry conditions. The codes for decomposing SWC with the SA and TA models and related EOF analysis were written in Matlab and are freely available from the authors upon request."

I was furthermore wondering why S_{tn} from the Parry and Niemann (2007) based model are not also correlated against the site factors (i.e. soil properties, slope, etc., see table 1). This would help to understand the differences between the two investigated approaches.

Response:

For the Parry and Niemann (2007) based model (i.e., the SA) model, two components were included in the S_{tn} , i.e., spatial mean $S_{\hat{t}n}$ and spatial anomaly Z_{tn} . The S_{tn} is the original soil water content. The spatial pattern of S_{tn} varied with time, and its controlling factors have been extensively analyzed before. The temporal series of spatial mean $S_{\hat{t}n}$ cannot be correlated with site factors. So, we guess you mean the correlation between the underlying spatial pattern of Z_{tn} and site factors.

Actually, we did correlate the underlying spatial pattern (i.e., EOF1) of Z_{tn} from the Parry and Niemann (2007) to the site factors. However, the controls of EOF1 in Z_{tn} were the same as those of $M_{\hat{t}n}$. This was because the spatial pattern of EOF1 in the Z_{tn} was identical to the time-stable patterns $M_{\hat{t}n}$ in the TA model as also reflected by the correlation coefficient of 1 between EOF1 of Z_{tn} and time-stable pattern $M_{\hat{t}n}$. Because of this reason, we did not show the correlation coefficients between EOF1 in the Z_{tn} and site factors.

This has been explained at L3-6 of Page 6478 in previous copy " **Correlation analysis indicated that the spatial pattern of EOF1 in the Z_{tn} was identical to the time-stable**

patterns ($M_{\hat{m}}$) in the TA model ($R=1.0$). The controls of EOF1 was therefore the same as those of $M_{\hat{m}}$, and will be discussed later. "

Then a comment on section 2.3: does the performance of TA and SA not mainly depend on how well the respective ECs can be reproduced by the fitted function? I have the impression that the scatter in the S_{tn} – EC1 relationship is reduced for TA. . . may this be interpreted as such that the TA pre-filters more of the variance from the original data? But then, in a distant future, it may be desired to estimate the EOFs for ungauged catchments from a (future) database with data from water content observation networks, in a similar as done with pedotransfer functions. However, in the case of the TA, one more spatial distribution would have to be estimated. This is certainly not an advantage. Could you comment on this?

Response:

(1) We agree with you that the goodness of fit for the relationship between EC1 and $S_{\hat{m}}$ is also one factor influencing the performance of TA and SA. The percentages in amount of the variances in EC1 explained by the cosine function was a bit higher for the TA than the SA model. For example, $R^2=0.76$ at the near surface and 0.88 in the root zone for the TA model, while $R^2=0.73$ in both the near surface and root zone for the SA model. So, the reduced scatter in the EC1 and $S_{\hat{m}}$ relationship in TA may also explain partly the outperformance of TA over SA. This was added at Lines 580-584:

" The relationship between the $S_{\hat{m}}$ and EC1 was better fitted by the cosine function in the TA model than the SA model (Figs. 4b and 6b), with R^2 of 0.76 versus 0.73 in the near surface and 0.88 versus 0.73 in the root zone. The reduced scatter in the $S_{\hat{m}}$ and EC1 relationship for the TA model may also partly explain the outperformance of the TA model over the SA model."

But we cannot conclude that the performance of the TA and the SA models MAINLY depend on how well the respective ECs can be reproduced by the fitted function. If this was the truth, the outperformance of TA over SA in the root zone should be more obviously than that in the near surface because the scatters for the two models were similar for the surface layer and the scatter of the TA model was much less than the SA model in the root zone. However, according to Fig.9, the outperformance of the TA model over the SA model was comparable between the near surface and root zone. Therefore, as we discussed in the discussion (Lines 585-594),

" the outperformance of the TA model over the SA model depends on counterbalance among the variance of R_{tn} explained in the TA model, the linear correlation between the $M_{\hat{tn}}$ and EOF1 of the R_{tn} , and the goodness of fit for the $S_{\hat{tn}}$ and EC1 relationship. For example, the variance of EOF1 in the R_{tn} for the near surface (i.e., 264%²) was much greater than that for the root zone (i.e., 43%²). However, $M_{\hat{tn}}$ and underlying spatial patterns (EOF1) in the R_{tn} in the root zone deviated more from a linear relationship, and the reduced scatter in the $S_{\hat{tn}}$ and EC1 relationship in the TA model was more obviously in the root zone than in the near surface. As a result, the outperformance of the TA model was comparable between the near surface and root zone at the Canadian site (Fig. 9)."

(2) We agree that the TA model is more complex than the SA model because one more spatial distribution has to be estimated. But on the other hand, estimation error is another factor that should be considered. Therefore, both model complexity and prediction errors should be taken into account during the model selection. This is why we introduced the AICc index to evaluate the two models. From the SWC data from the Canadian prairies, we found that when all 23 datasets were used and only EOF1 was considered, the TA model had lower AICc values than the SA model (please see L2-5 at Page 6481 in the previous copy). This indicated that even when penalty to complexity was given, the TA model was better than the SA model. Also considering that parameters in both models are estimated based on the same soil water content observation network, the TA model can be advantageous in case soil water distribution can be much better estimated.

However, as we added in the conclusions part (Lines 634-640): "**Therefore, the future study should be directed to estimate spatially distributed SWC in un-gauged watersheds based on the estimation of the model parameters using pedotransfer functions. Since the TA model needs one more spatial parameter (i.e., $M_{\hat{tn}}$) than the SA model, the advantage of the TA model may be weakened. Nevertheless, the TA model may be preferred if it estimates spatial SWC much better than the SA model such as under dry conditions.**"

Finally, for the sake of clarity, I suggest to expand the sentence on P6472,L14-16 and convert it in a little section on how the site properties were compared to which model parameters. This section would nicely fit in before section 2.3. Also the multiple stepwise regressions used in table 1 should be mentioned here.

Otherwise I only have some specific comments. I recommend a publication of hessd-12-6467-2015 after revisions

Response:

The sentence " These properties were used to relate time-stable patterns and underlying spatial patterns of space-variant temporal anomaly to environmental factors." on P6472, L14-16 was removed. We mentioned all the properties we used for correlation analysis at Lines 149-154 as:

" These properties included soil particle components (clay, silt, and sand contents), bulk density, soil organic carbon (SOC) content for the surface layer, A horizon depth, C horizon depth, depth to the CaCO₃ layer, leaf area index, elevation, cos(aspect), slope, curvature, gradient, upslope length, solar radiation, specific contributing area, convergence index, wetness index, and flow connectivity. Detailed information on the measurements can be found in Biswas et al. (2012)."

We expanded this sentence in a paragraph immediately before section 2.3. The multiple stepwise regressions were also mentioned here. Therefore, we added a paragraph right before section 2.3 as (Lines 260-265):

" The Pearson correlation coefficient (R) is used to explore the linear relationships between various spatial components in the two models (i.e., EOF1 of the Z_{tn} in the SA model, M_{in} , and EOF1 of the R_{tn} in the TA model) and environmental factors (i.e., soil, vegetative, and topographical properties). The multiple stepwise regressions are conducted to determine the percentage of variations in the spatial components which the controlling factors explain. "

Specific comments P6468L4-6: this sentence disconnects the sentences before and after which belong together. It is difficult to understand what is meant. I would rephrase it.

Response:

We changed the first sentences (L2-9 at Page 6468) as (Lines 8-15):

" A model was used to decompose the spatiotemporal SWC into a time-stable pattern (i.e., temporal mean), a space-invariant temporal anomaly, and a space-variant temporal anomaly. The space-variant temporal anomaly was further decomposed using the empirical orthogonal function (EOF) for estimating spatially distributed SWC. This model was compared to a previous model that decomposes the spatiotemporal SWC into a spatial

mean and a spatial anomaly, with the latter being further decomposed using the EOF. These two models are termed temporal anomaly (TA) model and spatial anomaly (SA) model, respectively. "

P6470L2 and L3: "may be further"?

Response:

Yes. we changed " be further" to "may be further" for both L2 and L3 on Page 6470.

Section 2.1.: I suggest presenting the study area in more detail and include soil textures, elevation differences and vegetation. It would be also nice to be informed about the CaCO₂ layer before it is discussed in the material and methods.

Response:

We added more information on elevation differences, soil textures, and vegetation at Lines 129-132:

" The elevation varies from 554.8 to 557.5 m. The soils are dominated by clay loam textured Mollisols (Soil Survey Staff, 2010) and covered by mixed grass, i.e., smooth brome grass (*Bromus inermis*) and alfalfa (*Medicago sativa* L.). "

The information on CaCO₃ layer was also added at Lines 133-137:

" Calcium carbonates (CaCO₃) derived mostly from fragments of limestone rocks are common in the Canadian Prairies. The CaCO₃ is dissolved by the slightly acidic rainwater moving through the upper horizons and deposited to lower horizons. The heterogeneous amount of infiltrated water resulted in a varying depth of CaCO₃ layer ranging from almost 0 m in the knolls to 2.1 m in the depressions. "

Section 2.2.: I found this section contains many long sentences, some of which are formulated in a misleading way.

Response:

We checked and revised this section to try to avoiding misunderstanding. This section was changed as (Lines 155-265) :

2.2 Statistical models for decomposing soil water content

Spatiotemporal SWC at small watershed scales was decomposed into three components: time-stable pattern, space-invariant temporal anomaly, and space-variant temporal anomaly. This model was compared to the one that decomposed SWC into spatial mean and spatial anomaly (Perry and Niemann, 2007). Both the space-variant temporal anomaly and spatial anomaly were decomposed using the EOF method. The two models are termed temporal anomaly (TA) model and spatial anomaly (SA) model, respectively. Figure 1 displays the differences between the two models. Each component will be explained in detail later. The explanation of nomenclatures is listed in Table A1. Because we focus on estimating spatial distribution of SWC at any given time, only spatial variances of SWC were taken into account. Therefore, the variance or covariance denotes the quantity in space without specifications.

2.2.1 The SA model

Perry and Niemann (2007) expressed SWC at location n and time t (S_{tn}) as (Fig. 1):

$$S_{tn} = S_{t\hat{n}} + Z_{tn}, \quad (1)$$

where $S_{t\hat{n}}$ is the spatial mean SWC at time t (temporal forcing) and Z_{tn} is the spatial anomaly of SWC (lumped spatial forcing and interactions). The subscript \hat{n} (\hat{t}) indicates a space (time) averaged quantity.

According to Perry and Niemann (2007), $S_{t\hat{n}}$ can be estimated by remote sensing, water balance models, and in situ soil water measurement at a representative (or time-stable) location. The in situ soil water measurement method was selected because the representative location can be easily determined with prior SWC datasets. By measuring

SWC only at the most time-stable location (s) and future time t (S_{ts}), $S_{\hat{m}}$ can be estimated using (Grayson and Western, 1998):

$$S_{\hat{m}} = \frac{S_{ts}}{1 + \delta_{ts}^*}, \quad (2)$$

where the s was identified using the time stability index of mean absolute bias error (Hu et al., 2010, 2012). The δ_{ts}^* is the temporal mean relative difference of SWC at the s , which was calculated with prior measurements.

Spatial anomaly (Z_{tm}) can be reconstructed by the sum of the product of time-invariant spatial structures (EOFs) and temporally varying coefficients (ECs) using the EOF method (Perry and Niemann, 2007; Joshi and Mohanty, 2010; Vanderlinden et al., 2012). The ECs correspond to the eigenvectors of the matrix of spatial covariance of the Z_{tm} , and the EOFs are obtained by projecting the Z_{tm} onto the matrix ECs as: $\text{EOFs} = Z_{tm} \text{ECs}$. The number of EOF (or EC) series equals the number of sampling dates. Each EOF series corresponds to one value at each location, and each EC series has one value at each measurement time. Each EOF is chosen to be orthogonal to other EOFs, and the lower-order EOFs account for as much variance as possible. The sum of variances of all EOFs equals the sum of variances of Z_{tm} from all measurement times.

Usually, a substantial amount of variance can be explained by a small number of EOFs. Johnson and Wichern (2002) suggested the eigenvalue confidence limits method for selecting the number of EOFs. Once the number of significant EOFs at a confidence level of

95% is selected, Z_{tm} can be estimated as the sum of the product of significant EOFs and associated ECs as:

$$Z_{tm} = \sum \text{EOF}^{sig} \times (\text{EC}^{sig})^T, \quad (3)$$

where EOF^{sig} represents the significant EOFs of the Z_{tm} obtained during model development, EC^{sig} is the associated temporally varying coefficient, and the superscript T represents matrix transpose. Following Perry and Niemann (2007), the associated significant EC at time t (EC_t), is estimated by the cosine relationship between EC and $S_{\hat{m}}$ developed using prior measurements:

$$\text{EC}_t = a + b \cos\left(\frac{2\pi}{c} S_{\hat{m}} - d\right), \quad (4)$$

where a , b , c , and d are the fitted parameters using prior measurements and $S_{\hat{m}}$ is estimated from Eq. (2). By using the continuous function, EC_t can be estimated at any $S_{\hat{m}}$ values, which allows for the estimation of spatially distributed SWC at any soil water conditions.

2.2.2 The TA model

Mittelbach and Seneviratne (2012) decomposed the S_m into a time-stable pattern (i.e., temporal mean) and a temporal anomaly component (Fig. 1):

$$S_m = M_{\hat{m}} + A_m, \quad (5)$$

where $M_{\hat{m}}$ is the time-stable pattern (spatial forcing) controlled by “static” factors such as soil properties and topography; A_m refers to the temporal anomaly (lumped temporal forcing and interactions). The variance of SWC ($\sigma_{\hat{n}}^2(S_m)$) is the sum of variance of the $M_{\hat{m}}$ ($\sigma_{\hat{n}}^2(M_{\hat{m}})$), variance of the A_m ($\sigma_{\hat{n}}^2(A_m)$), and two times of covariance between $M_{\hat{m}}$ and A_m ($2\text{cov}(M_{\hat{m}}, A_m)$), which can be expressed as:

$$\sigma_{\hat{n}}^2(S_m) = \sigma_{\hat{n}}^2(M_{\hat{m}}) + 2\text{cov}(M_{\hat{m}}, A_m) + \sigma_{\hat{n}}^2(A_m). \quad (6)$$

Because the A_m in Mittelbach and Seneviratne (2012) is a lumped term, it can be further decomposed into space-invariant temporal anomaly ($A_{\hat{m}}$, i.e., temporal forcing) and space-variant temporal anomaly (R_m , i.e., interactions) (Vanderlinden et al., 2012). At a watershed scale, the $A_{\hat{m}}$ is controlled by temporally varying factors such as meteorological variables and vegetation. Positive and negative $A_{\hat{m}}$ correspond to relatively wet and dry periods, respectively. The R_m refers to the redistribution of $A_{\hat{m}}$ among different locations due to the interactions between spatial forcing and temporal forcing. For example, soil and topography regulate how much rainfall enters soil and how much water runs off or runs on at a location. This, in turn, dictates vegetation growth in a water-limited environment. Therefore, S_m can also be expressed as (Fig. 1):

$$S_m = M_{\hat{m}} + A_{\hat{m}} + R_m. \quad (7)$$

The temporal trends of $A_{\hat{m}}$ in Eq. (7) and $S_{\hat{m}}$ in Eq. (1) are the same as both represent temporal forcing. Because the $A_{\hat{m}}$ is space-invariant and orthogonal to the $M_{\hat{m}}$ and R_m in a space, $\sigma_{\hat{n}}^2(S_m)$ in Eq. (6) can also be written as:

$$\sigma_{\hat{n}}^2(S_m) = \sigma_{\hat{n}}^2(M_{\hat{in}}) + 2\text{cov}(M_{\hat{in}}, R_m) + \sigma_{\hat{n}}^2(R_m), \quad (8)$$

where $\text{cov}(M_{\hat{in}}, R_m)$ is the covariance between the $M_{\hat{in}}$ and R_m , and $\sigma_{\hat{n}}^2(R_m)$ is the variance of the R_m . Apparently, $2\text{cov}(M_{\hat{in}}, R_m)$ equals $2\text{cov}(M_{\hat{in}}, A_m)$, and $\sigma_{\hat{n}}^2(R_m)$ equals $\sigma_{\hat{n}}^2(A_m)$. The percent (%) contributions of $\sigma_{\hat{n}}^2(M_{\hat{in}})$, $2\text{cov}(M_{\hat{in}}, R_m)$, and $\sigma_{\hat{n}}^2(R_m)$ to the $\sigma_{\hat{n}}^2(S_m)$ are calculated. The $\text{cov}(M_{\hat{in}}, R_m)$ can be negative at some conditions, for example, when the depressions correspond to greater $M_{\hat{in}}$ and more negative R_m values in the discharge periods. This resulted in percentage contributions of $\sigma_{\hat{n}}^2(M_{\hat{in}})$ and $\sigma_{\hat{n}}^2(R_m) > 100\%$ and percentage contributions of $2\text{cov}(M_{\hat{in}}, R_m) < 0\%$ (Mittelbach and Seneviratne, 2012; Brocca et al., 2014; Rötzer et al., 2015). If R_m is zero at any time or location, there are no interactions between spatial forcing and temporal forcing, $\sigma_{\hat{n}}^2(S_m)$ and the spatial trends of SWC are consistent over time. Therefore, R_m is directly responsible for temporal change in the spatial variability of SWC.

If some underlying spatial patterns exist in R_m , R_m can be reconstructed by the sum of the product of time-invariant spatial structures (EOFs) and time-dependent coefficients (ECs) using the EOF method. Note that the number of EOF (or EC) series also equals the number of sampling dates.

For estimation of spatially distributed SWC, R_m is estimated by the same method as Z_m using Eq. (3). The $M_{\hat{in}}$ is estimated with prior measurements by:

$$M_{\hat{in}} = \frac{1}{m} \sum_{j=1}^m S_m, \quad (9)$$

where m is the number of previous measurement times, and $A_{\hat{m}}$ is estimated by:

$$A_{\hat{m}} = S_{\hat{m}} - M_{\hat{m}}, \quad (10)$$

where $M_{\hat{m}}$ is the spatial mean of M_m , and $S_{\hat{m}}$ is estimated from SWC measurements at the most time-stable location using Eq. (2).

The Pearson correlation coefficient (R) is used to explore the linear relationships between various spatial components in the two models (i.e., EOF1 of the Z_m in the SA model, $M_{\hat{m}}$, and EOF1 of the R_m in the TA model) and environmental factors (i.e., soil, vegetative, and topographical properties). The multiple stepwise regressions are conducted to determine the percentage of variations in the spatial components which the controlling factors explain."

Equation (2): In this point the SA method deviates from the one described in Perry and Niemann (2009). Please point this out and explain and justify why you preferred to estimate $S_{\hat{m}}$ in this way.

Response:

Actually, in the study of Perry and Niemann (2009), they did not estimate the mean soil water content but instead use the true value of mean soil water content for estimating soil water distribution. Meanwhile, they discussed how to estimate the mean soil water content. As we added in the revision (Lines 174-176):

" According to Perry and Niemann (2007), $S_{\hat{m}}$ can be estimated by remote sensing, water balance models, and in situ soil water measurement at a representative (or time-stable) location. "

From Perry and Niemann (2009), we can find that they put more paragraphs on the discussion of the later (i.e., third) method. Therefore,

" The in situ soil water measurement method was selected because the representative location can be easily determined with prior SWC datasets. By measuring SWC only at the most time-stable location (s) and future time t (S_{ts}), $S_{\hat{m}}$ can be estimated using (Grayson and Western, 1998):

$$S_{\hat{m}} = \frac{S_{ts}}{1 + \delta_{ts}}, \quad (2)$$

where the s was identified using the time stability index of mean absolute bias error (Hu et al., 2010, 2012). The δ_{ts} is the temporal mean relative difference of SWC at the s , which was calculated with prior measurements." (Lines 176-183).

Different locations provide different accuracy of spatial average soil moisture. There are many indices which can be used to determine the best location. According to Hu et al. (2010, 2012), the mean absolute bias error is the best index to identify the most time-stable location for estimating the spatial average soil moisture. This is why we used Eq. (2) to estimate spatial average soil water content.

In summary, we used one of the methods that Perry and Niemann (2007) mentioned. As Perry and Niemann (2007) mentioned, the spatial average soil moisture for the near surface can also be estimated by the remote sensed SWC, and this is why we mentioned that "**If the TA model parameters (i.e., $M_{\hat{m}}$, EOF1 of the $R_{\hat{m}}$, and relationship between EC and $S_{\hat{m}}$) are obtained from historical SWC datasets, a detailed spatially distributed SWC of near surface soil at watershed scales can be constructed from remote sensed SWC.**" (Lines 630-633). This also answered one comment made the Referee #2.

P6473L15-P6474L4: see remark on section 2.2. I only understood what was meant in this section after reading Perry and Niemann (2007). It is for example not clear from the text why the abbreviation of EC is used and that EC corresponds to the matrix of eigenvectors. The manuscript would gain considerably if this passage was better explained.

Response:

Please see the response about the comments on section 2.2.

We explained these paragraphs in more detail. Therefore, we revised these paragraphs as (Lines 184-194):

" Spatial anomaly ($Z_{\hat{m}}$) can be reconstructed by the sum of the product of time-invariant spatial structures (EOFs) and temporally varying coefficients (ECs) using the EOF method (Perry and Niemann, 2007; Joshi and Mohanty, 2010; Vanderlinden et al., 2012). The ECs correspond to the eigenvectors of the matrix of spatial covariance of the

Z_{tm} , and the EOFs are obtained by projecting the Z_{tm} onto the matrix ECs as:

EOFs = Z_{tm} ECs . The number of EOF (or EC) series equals the number of sampling dates.

Each EOF series corresponds to one value at each location, and each EC series has one value at each measurement time. Each EOF is chosen to be orthogonal to other EOFs, and the lower-order EOFs account for as much variance as possible. The sum of variances of all EOFs equals the sum of variances of Z_{tm} from all measurement times. "

Equation (4): Please also explain shortly why it is necessary to approximate ECt by a continuous function

Response:

We approximate ETc with the cosine function for two reasons:

First, in the SA method, Perry and Niemann (2007) used the continuous function. We did the same thing for keeping consistency.

Second, by using the continuous function, EC_t can be estimated at any S_{in} values, which allows for the estimation of spatially distributed SWC at any soil water conditions.

Therefore, we changed the related paragraph as (Lines 203-210):

" Following Perry and Niemann (2007), the associated significant EC at time t (EC_t), is estimated by the cosine relationship between EC and S_{in} developed using prior measurements:

$$EC_t = a + b \cos\left(\frac{2\pi}{c} S_{in} - d\right), \quad (4)$$

where a , b , c , and d are the fitted parameters using prior measurements and S_{in} is estimated from Eq. (2). By using the continuous function, EC_t can be estimated at any S_{in} values, which allows for the estimation of spatially distributed SWC at any soil water conditions."

P6479L8 and following: Percent of what? How can something contribute to another thing by more than 100%? What are %² (Figure 5)? It needs to be explained in the material and methods what “percents” is referring to.

Response:

We used the "%" as a unit for two quantity in this manuscript.

First, it was used to express the percent (%) of $\sigma_{\hat{n}}^2(M_{\hat{in}})$, $2\text{cov}(M_{\hat{in}}, R_m)$, and $\sigma_{\hat{n}}^2(R_m)$ to the total variance of SWC, $\sigma_{\hat{n}}^2(S_m)$. So, it is the percent of the $\sigma_{\hat{n}}^2(S_m)$. We understand that it is weird to say something contribute to another thing by more than 100%. But as we added at Lines 240-245: "**The $\text{cov}(M_{\hat{in}}, R_m)$ can be negative at some conditions, for example, when the depressions correspond to greater $M_{\hat{in}}$ and more negative R_m values in the discharge periods. This resulted in percentage contributions of $\sigma_{\hat{n}}^2(M_{\hat{in}})$ and $\sigma_{\hat{n}}^2(R_m) > 100%$ and percentage contributions of $2\text{cov}(M_{\hat{in}}, R_m) < 0%$ (Mittelbach and Seneviratne, 2012; Brocca et al., 2014; Rötzer et al., 2015).**". Considering that previous studies on this topic used the same terminology, we just explained how these percentages can be more than 100% to avoid confusion.

Second, "**The SWC was measured on a volumetric basis and expressed as a percentage (%) volume of water per unit soil volume.**" (Lines 142-143). So the variance of soil water content should have the unit of %².

P6479L18: arithmetic average?

Response:

Yes. we changed "average" to "arithmetic average".

P6481L19: These values do not fit to the y-axes of figure 7. Please adapt. Please also call out figure 8 already at this point.

Response:

Sorry, we made a mistake here, the value "4.05" should be "-4.05". We did not plot these data in Figure 7. In Figure 8, as we mentioned in the caption: "**At 0–0.2 m, negative Nash-Sutcliffe coefficient of efficiency values for three dates (October 22, 2008, August 27, 2009, and October 27, 2009) are not shown**". This is done for better displaying the NSCE values for other dates.

P6483L2: Please be more specific with what you mean by “needed”.

Response:

What we mean here is only EOF1 should be considered for estimating spatially distributed SWC because EOF2 and EOF3 contributed little to the SWC estimation. We changed the related sentence to:

" Although three significant EOFs of the R_{tn} existed in some cases, only EOF1 rather than higher-order EOFs of the R_{tn} should be considered for the spatially distributed SWC estimation." (Lines 511-513).

Interactive comment on “Estimating spatially distributed soil water content at small watershed scales based on decomposition of temporal anomaly and time stability analysis” by W. Hu and

B. C. Si

Anonymous Referee #2

Received and published: 5 August 2015

Overview

The study describes a new approach (likely better “new concept”) for investigating spatial-temporal variability of soil moisture at catchment scale. Specifically, the decomposition of spatiotemporal soil moisture patterns in three components was carried out: temporal mean, space-invariant temporal anomaly, and space-variant temporal anomaly. The new model (TA) was compared with the approach (SA) by *Perry and Niemann (2007)* who decomposed spatiotemporal soil moisture patterns into spatial mean and spatial anomaly. By using in situ observations from a transect in the Canadian Prairies, the authors obtained that TA model performs better than SA model, mainly in dry conditions in which the variability of the space-variant temporal anomaly is stronger.

General Comments

I found the paper well written, well-structured and clear. I also believe the topic is of interest for the readers of HESS as it describes a new concept for analysing spatiotemporal soil moisture patterns, based on new understanding of the different components driving soil moisture variability.

However, I believe that one aspect (method presentation) should be improved and I have two major comments to be addressed before the publication.

Response:

Thank you for reviewing our manuscript and your constructive comments. Please refer to all changes in the revised manuscript following our response.

MINOR COMMENT: The method is well-written, but still quite complex to be understood. By using a soil moisture dataset I have collected, I tried to visualize the different components in a 2D plot (see e.g., *Fig. 1*). Hoping to be correct, from the figure it’s easier for me to understand how the SA and TA models work. I believe that this kind of visualization will facilitate the readers.

Response:

Thank you. We removed Fig.2 and 4 in the previous copy, and combine them in one figure (Fig. 3) as you suggested. Meanwhile, we put the meteorological data in Fig. 2 (see below).

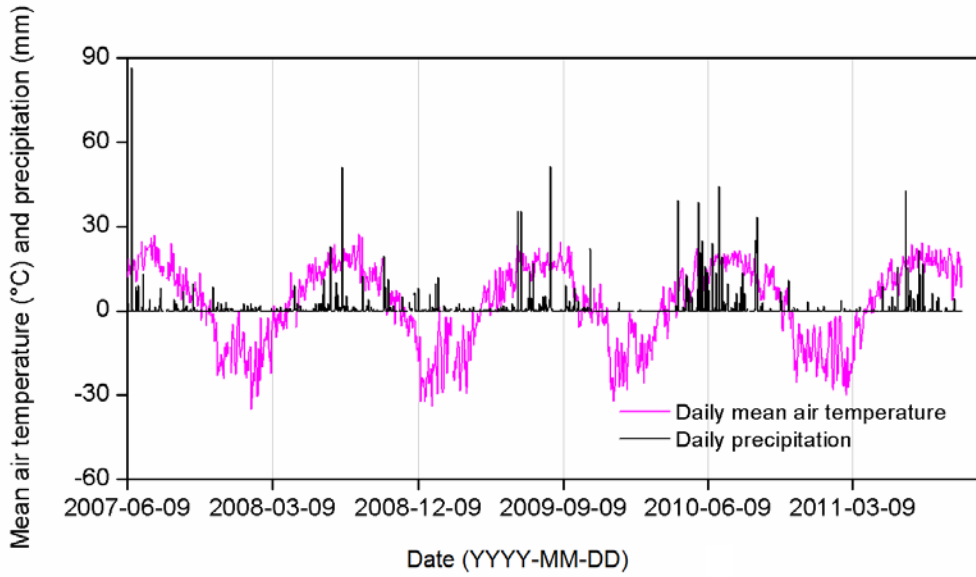


Figure 2. Daily mean air temperature and precipitation during the study period.

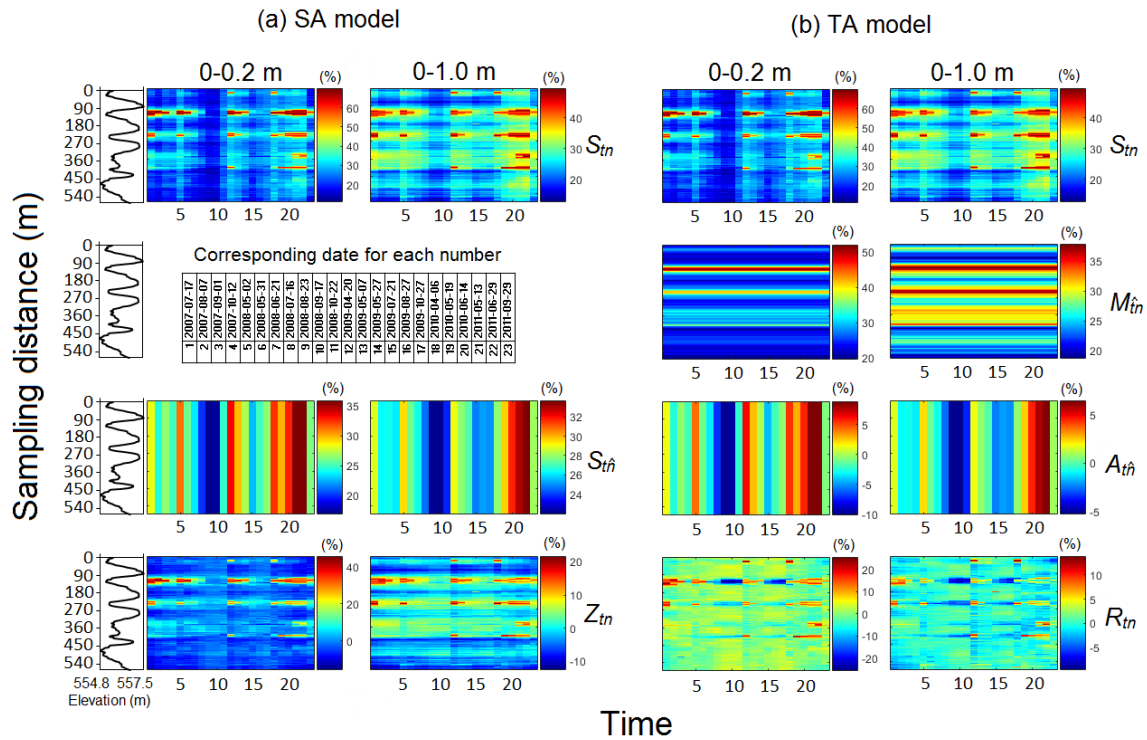


Figure 3. Components of soil water content in (a) the SA model (spatial mean soil water content $S_{\hat{in}}$ and spatial anomaly $Z_{\hat{in}}$) and in (b) the TA model (time-stable pattern $M_{\hat{in}}$, space-invariant

temporal anomaly $A_{\hat{n}}$, and space-variant temporal anomaly R_m) for 0–0.2 and 0–1.0 m. Also shown is the elevation.

MAJOR COMMENT: Only one study site is used to test the SA and TA models. Even though I am aware that the main purpose of the paper is the presentation of the “new concept” (TA model), I believe that the analysis for a different test site might be added. The dataset of the Canadian Prairies is quite famous (I have in mind at least 6 papers that makes use of this dataset), and the correlation between topographic and soil data with soil moisture for this dataset is well-known. I was wondering what could happens if a different dataset were employed (freely available or collected by the authors).

Response:

We added two other datasets, one from **A hillslope in the Chinese Loess Plateau (Hu et al., 2011), and one from the GENCAI network in Italy (Brocca et al., 2012, 2013)**. Both datasets have been published and cited in this revision. The two datasets, respectively, represent a smaller and larger scale than the Canadian site. Our results indicate that the TA model outperformed the SA model at the Chinese site and they were identical at the Italian site (Please see the detailed results below). The outperformance of the TA model at small scales (Chinese site and Canadian site) can be attributed to the existence of underlying spatial patterns in the R_m , while the absence of underlying spatial patterns in the R_m was the main reason why TA model was identical to that of the SA model at the Italian site. Similarly, because the first underlying spatial pattern (i.e., EOF1) explained greater percentages of the $\sigma_n^2(R_m)$ at the Canadian site (44–61%) than the Chinese site (23%), the outperformance of the TA model over the SA model was more obvious at the former site (Fig. 9 and 10a). The related discussion was made in the Discussion section 4.2. By using the different datasets, it is easier to understand under which circumstance the TA model is preferable to the SA model for estimating spatially distributed SWC.

" 3.3 Further application at other two sites with different scales

3.3.1 A hillslope in the Chinese Loess Plateau

Along a hillslope of 100 m in length in the Chinese Loess Plateau, SWC of 0–0.06 m was measured 136 times from June 25, 2007 to August 30, 2008 by a Delta-T Devices Theta

probe (ML2x) at 51 locations (Hu et al., 2011). The hillslope was covered by *Stipa bungeana* Trin. and *Medicago sativa* L. in sandy loam and silt loam soils. On average, the $\sigma_{\hat{n}}^2(M_{\hat{m}})$, $\sigma_{\hat{n}}^2(R_m)$, and $2\text{cov}(M_{\hat{m}}, R_m)$ contributed 53, 74 and -27% to the $\sigma_{\hat{n}}^2(S_m)$, indicating that both time-stable pattern and temporal anomalies were the main contributors to the $\sigma_{\hat{n}}^2(S_m)$. The EOF analysis showed that only the EOF1 was statistically significant for both the R_m and Z_m , and the EOF1 explained 23% and 47% of the total variances of R_m and Z_m , respectively. This illustrated that underlying spatial patterns exist in the R_m on the hillslope. Cross validation was used to estimate the spatially distributed SWC along the hillslope. The results showed that the NSCE varied from -4.25 to 0.83 (TA model) and from -4.30 to 0.81 (SA model), with a mean value of 0.25 and 0.18, respectively. A paired samples T-test showed that the NSCE values for the TA model were significantly ($P < 0.05$) greater than those for the SA model, indicating that the TA model outperformed the SA model. As Fig. 10a shows, the outperformance was greater when SWC deviated from intermediate conditions, especially for dry conditions, which was similar to the Canadian site.

3.3.2 The GENCAI network in Italy

In the GENCAI network (~250 km²) in Italy, SWC of 0–0.15 m was measured by a TDR probe at 46 locations, 34 times from February to December in 2009 (Brocca et al., 2012, 2013). The GENCAI area was dominated by grassland with a flat topography, in silty clay soils. The $\sigma_{\hat{n}}^2(M_{\hat{m}})$, $\sigma_{\hat{n}}^2(R_m)$, and $2\text{cov}(M_{\hat{m}}, R_m)$ contributed 38, 68, and -7% to the $\sigma_{\hat{n}}^2(S_m)$ (Brocca et al., 2014), indicating the dominant contribution of temporal anomalies on SWC variability. The first three EOFs of the R_m explained 19, 16, and 8% of the total $\sigma_{\hat{n}}^2(R_m)$, and no EOFs were statistically significant, indicating that no underlying spatial patterns exist in the R_m . The EOF1 of the Z_m was significant and accounted for 37% of

the variances in the Z_{in} . Although the EOF1 of the R_{in} was not significant, it was considered in the TA model for estimating spatially distributed SWC. The cross validation indicates that the NSCE varied from -0.79 to 0.50 (TA model) and from -0.87 to 0.56 (SA model), with mean values of 0.09 and 0.08, respectively. The SWC estimation based on these two models was not satisfactory except for a few days. As Fig. 10b shows, the differences in NSCE values between the two models were scattered around 0. A paired samples T-test showed that the NSCE values between the TA model and the SA model were not significant ($P < 0.05$), indicating no differences in estimating spatially distributed SWC between these two models. "

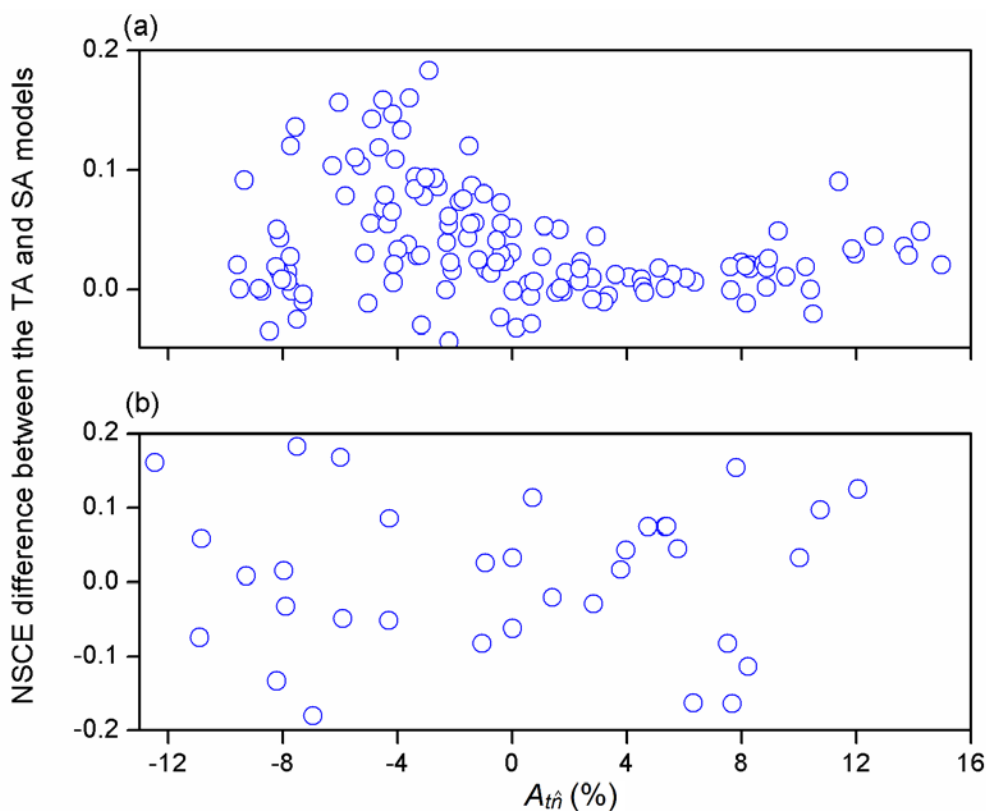


Figure 10. Difference between the Nash-Sutcliffe coefficient of efficiency (NSCE) of soil water content evaluation by the cross validation using the TA and SA models as a function of space-invariant temporal anomaly A_{tin} for (a) 0–0.06 m of the Chinese Loess Plateau hillslope and (b) 0–0.15 m of the GENCAI network in Italy.

MAJOR COMMENT: In the last sentence of the abstract it reads that “the TA model has potential to construct a spatially distributed SWC at watershed scales from remote sensed SWC.” Even

though it is potentially true, I believe that the paper makes only a first (short) step toward this interesting application. Indeed, for building the SA and TA models, the whole (spatially distributed) soil moisture dataset is used in the study.

Therefore, it was not demonstrated that TA (or SA) model provides good performance in reproducing spatial soil moisture pattern by using single measurements. At least, I suggest splitting the soil moisture dataset in a calibration and validation set. Otherwise, the models can be used only for understanding the different components driving soil moisture variability, not really as predictive tools (at least, it is not shown in the paper).

Response:

First, we have to clarify that we did use the whole SWC dataset for building the TA and SA model in order to display the different components of these two models and determine their controls. But when we estimated the spatial SWC using the cross validation method, **" an iterative removal of 1 of the 23 dates is made for model development, and the SWC along the transect corresponding to the removed date is estimated iteratively."** (Lines 273-275). From this aspect, we did evaluate the models in terms of reproducing spatial SWC by using independent measurements.

In this revision, we also used the external validation as you suggested for the main datasets (Canadian site). **"For the external validation, SWC from 14 dates of the first two years (from July 17, 2007 to May 27, 2009) is used for model development, and the SWC distribution of 9 dates in the second two years (from July 21, 2009 to September 29, 2011) is estimated."** (Lines 275-278).

" During the external validation, the TA model resulted in SWC estimations with NSCE values ranging from 0.61 to 0.85 near the surface and from 0.32 to 0.92 in the root zone, with exception of two days (August 27, 2009 and October 27, 2009 with NSCE values of -2.63 and -5.12, respectively) at 0–0.2 m (Fig. 8). This suggested that the TA model performed well in estimating spatially distributed SWC patterns except on August 27, 2009 and October 27, 2009 at 0–0.2 m. The estimation in the root zone was also generally better than in the near surface." (Lines 443-449).

" The difference in NSCE values between the TA and SA models for both validations are presented in Fig. 9. Generally, the difference decreased as $A_{\hat{n}}$ increased, and then slightly

increased with a further increase in $A_{\hat{m}}$. A paired samples T-test indicated that the NSCE values of the TA model were significantly ($P<0.05$) greater than those of the SA model for both soil layers, irrespective of validation methods. This indicates that the TA model outperformed the SA model, particularly in dry conditions. This was because when the soil was dry, there was a high contribution of $\sigma_{\hat{n}}^2(R_m)$, and thus strong variability in the space-variant temporal anomaly." (Lines 460-467).

Therefore, the external validation also supported the conclusion made by the cross validation. Because of this reason and for shortening the paragraph of this manuscript, we did not use external validation for the application of these two models to the other two sites.

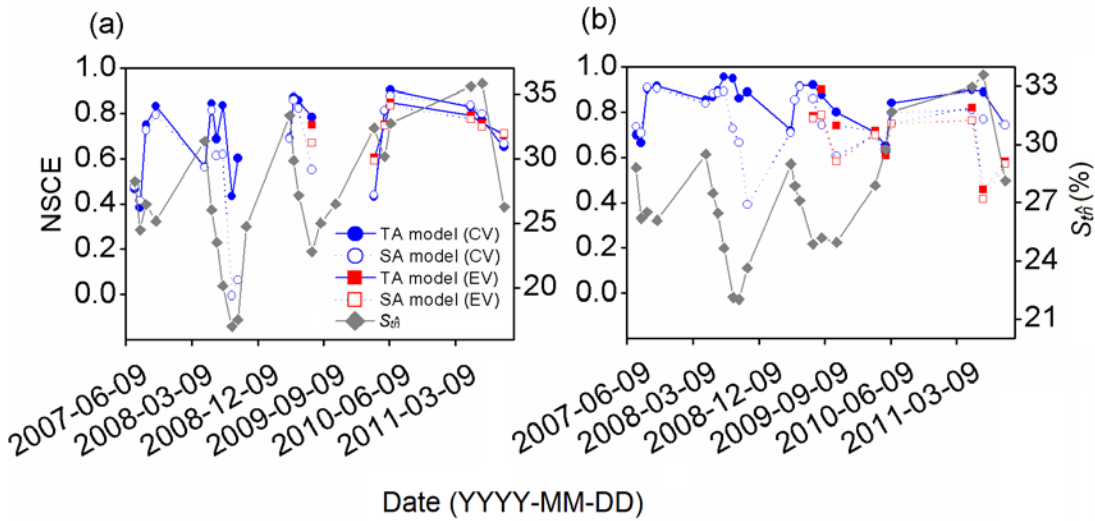


Figure 8. The Nash-Sutcliffe coefficient of efficiency (NSCE) of soil water content estimation using the TA and SA models for (a) 0–0.2 and (b) 0–1.0 m for both cross validation (CV) and external validation (EV). At 0–0.2 m, negative Nash-Sutcliffe coefficient of efficiency values for three dates (October 22, 2008, August 27, 2009, and October 27, 2009) are not shown. Spatial mean soil water content $S_{\hat{n}}$ on each measurement day is also shown.

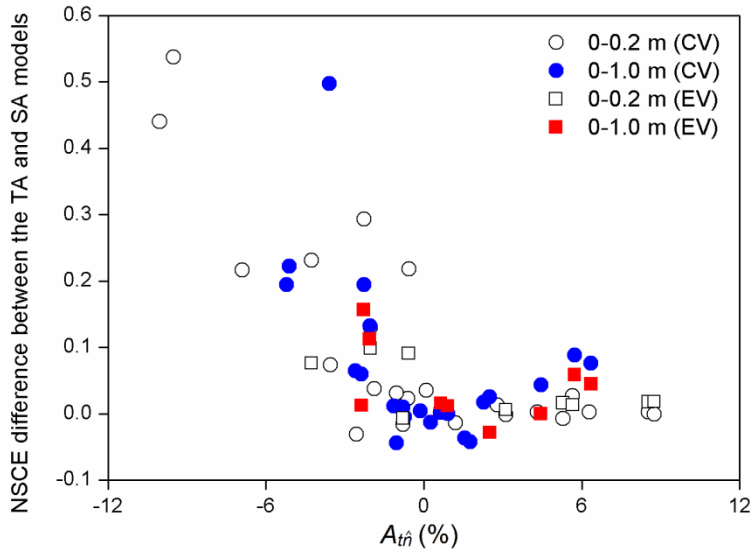


Figure 9. Difference between the Nash-Sutcliffe coefficient of efficiency (NSCE) of soil water content estimation by both cross validation (CV) and external validation (EV) using the TA and SA models as a function of space-invariant temporal anomaly $A_{\hat{t}n}$ for (a) 0–0.2 and (b) 0–1.0 m.

Moreover, it should be clarified how the authors believe to use the TA model to construct spatially distributed soil moisture from remote sensing observations.

Response:

As we answered above, spatial average SWC $S_{\hat{t}n}$ has to be estimated for estimating spatially distributed SWC. " According to Perry and Niemann (2007), $S_{\hat{t}n}$ can be estimated by remote sensing, water balance models, and in situ soil water measurement at a representative (or time-stable) location. ". In this manuscript, we used the later method to estimate the $S_{\hat{t}n}$.

As we revised the conclusion, " If the TA model parameters (i.e., $M_{\hat{t}n}$, EOF1 of the R_{tn} , and relationship between EC and $S_{\hat{t}n}$) are obtained from historical SWC datasets, a detailed spatially distributed SWC of near surface soil at watershed scales can be constructed from remote sensed SWC." (Lines 630-633).

As mentioned by the first reviewer, some polishing of the text should be given (e.g., at page 6481, line 19 it reads NSCE of 4.05 and it should be -4.05) but it can be easily accomplished by the authors through a careful rereading of the manuscript.

Response:

Sorry for the mistake. We have changed 4.05 to -4.05.

We checked the manuscript carefully during this revision.

1 Estimating spatially distributed soil water content at small watershed
2 scales based on decomposition of temporal anomaly and time stability
3 analysis

4 Wei Hu, Bing Cheng Si

5 *University of Saskatchewan, Department of Soil Science, Saskatoon, SK S7N 5A8, Canada*

6 **Abstract**

7 Soil water content (SWC) is crucial to rainfall-runoff response at the watershed scales
8 ~~is crucial to rainfall-runoff response~~. A model was used to decompose the
9 spatiotemporal SWC into a time-stable pattern (i.e, temporal mean), a space-invariant
10 temporal anomaly, and a space-variant temporal anomaly. The space-variant temporal
11 ~~anomaly or spatial anomaly was further decomposed using the empirical orthogonal~~
12 ~~function (EOF) for estimating spatially distributed SWC.~~ This model was compared
13 ~~with to~~ a previous model that decomposes the spatiotemporal SWC into a spatial
14 mean and a spatial anomaly, ~~with the latter being further decomposed using the EOF.~~
15 ~~The space-variant temporal anomaly or spatial anomaly was further decomposed~~
16 ~~using the empirical orthogonal function for estimating spatially distributed SWC.~~
17 These two models are termed temporal anomaly (TA) model and spatial anomaly (SA)
18 model, respectively. We aimed to test the hypothesis that underlying (i.e.,
19 time-invariant) spatial patterns exist in the space-variant temporal anomaly at the
20 small watershed scale, and to examine the advantages of the TA model over the SA
21 model in terms of the estimation of spatially distributed SWC. For this purpose, a

22 | ~~SWC~~ dataset of near surface (0–0.2 m) and root zone (0–1.0 m) ~~SWC, at~~from a small
23 | watershed scale in the Canadian prairies, was analyzed. Results showed that
24 | underlying spatial patterns exist in the space-variant temporal anomaly because of the
25 | permanent controls of “static” factors such as depth to the CaCO₃ layer and organic
26 | carbon content. Combined with time stability analysis, the TA model improved the
27 | estimation of spatially distributed SWC over the SA model ~~because the latter failed to~~
28 | ~~capture the space-variant temporal anomaly which accounted for non-negligible~~
29 | ~~amounts of spatial variance in SWC. The outperformance was greater when SWC~~
30 | ~~deviated from intermediate conditions~~, especially for dry conditions. Further
31 | application of these two models demonstrated that the TA model outperformed the SA
32 | model at a hillslope in the Chinese Loess Plateau, but the performance of these two
33 | models in the GENCAI network (~250 km²) in Italy was equivalent. ~~Therefore,~~ the
34 | TA model has potential to construct a spatially distributed SWC at small watershed
35 | scales from remote sensed SWC.

36 | Keywords: Soil moisture; Soil water downscaling; Empirical orthogonal function;
37 | Statistical models; Time stability

38 | 1. Introduction

39 | Soil water content (SWC) of surface soils exerts a major influence on a series of
40 | hydrological processes such as runoff and infiltration (Famiglietti et al., 1998;
41 | Vereecken et al., 2007; She et al., 2013a). Soil water content in of the root zone is,
42 | usually in many cases, linked to vegetative growth (Wang et al., 2012; Ward et al.,

2012; Jia and Shao, 2013). ~~Obtaining A~~accurate information on ~~the~~ spatiotemporal SWC is ~~cruciala prerequisite~~ for improving hydrological prediction and soil water management (Venkatesh et al., 2011; Champagne et al., 2012; She et al., 2013b; Zhao et al., 2013). While remote sensing has advanced SWC measurements of surface soils (<5 cm thick) at basin (2,500–25,000 km²) and continental scales (Robinson et al., 2008), characterization of spatially distributed SWC at small watershed (0.1–80 km²) scales still poses a challenge. A method is needed for estimating spatially distributed SWC in the near surface and root zone at watershed scales.

Time stability of SWC, ~~which referring-refers~~ to similar spatial patterns of SWC across different measurement times (Vachaud et al., 1985; Brocca et al., 2009), has been used for estimating spatially distributed SWC (Starr, 2005; Perry and Niemann, 2007; Blöschl et al., 2009). This method is conceptually-appealing, but assumes completely time-stable spatial patterns of SWC.

The time-stable pattern does not explain all of the spatial variances in SWC, indicating the existence of time-variant components (Starr, 2005). In order to identify underlying patterns of SWC that have time-variant components, ~~the~~ spatiotemporal SWC was decomposed into ~~a~~ spatial mean and ~~a~~ spatial anomaly~~-. The spatial anomaly of the SWC with the latter being~~as further decomposed into the sum of the product of time-invariant spatial patterns (EOFs) and temporally varying, but spatially constant coefficients (ECs) ~~by-using~~ the empirical orthogonal function (EOF) (Fig. 1) (Jawson and Niemann, 2007; Perry and Niemann, 2007, 2008; Joshi and Mohanty, 2010; Korres et al., 2010; Busch et al., 2012). Spatially distributed SWC estimates

65 based on the decomposition of spatial anomaly outperformed those based on
66 time-stable patterns (Perry and Niemann, 2007).

67 Recently, the spatiotemporal SWC was also decomposed into a temporal mean and
68 a temporal anomaly (Mittelbach and Seneviratne, 2012) (Fig. 1). Previous studies
69 indicated that the contribution of the temporal anomaly to the total spatial variance
70 was notable (Mittelbach and Seneviratne, 2012; Brocca et al., 2014; Rötzer et al.,
71 2015). These studies, however, only focused on surface soils ~~and-at~~ large scales (>
72 250 km²). Vanderlinden et al. (2012) suggested that the temporal mean may be further
73 decomposed into its spatial mean and residuals, and the temporal anomaly may be
74 further decomposed into space-invariant term (i.e., spatial mean of temporal anomaly)
75 and space-variant term (i.e., spatial residuals of temporal anomaly) (Fig. 1). Note that
76 the spatial variance in the temporal anomaly (Mittelbach and Seneviratne, 2012)
77 equals that ~~in-of~~ the space-variant term of the temporal anomaly (Vanderlinden et al.,
78 2012). The further decomposition of the temporal anomaly may be physically
79 meaningful, because the space-invariant and space-variant terms in the temporal
80 anomaly may be forced differently. However, the models of Mittelbach and
81 Seneviratne (2012) and Vanderlinden et al. (2012) have not been used for estimating
82 spatially distributed SWC. If the space-variant terms are ignored during the estimation
83 of spatially distributed SWC, their models are equivalent to that based on time-stable
84 patterns. Therefore, estimation of spatially distributed SWC may be improved by
85 incorporating the space-variant term of the temporal anomaly if underlying (i.e.,
86 time-invariant) spatial patterns exist in ~~#~~the temporal anomaly.

87 | To our knowledge, the importance of the space-variant term of the temporal
88 anomaly and its physical meaning at small watershed scales is not well-known. Based
89 on previous studies (Perry and Niemann, 2007; Mittelbach and Seneviratne, 2012;
90 Vanderlinden et al., 2012), we assume soil water dynamics at watershed scales can be
91 decomposed into three components (Fig. 1): (1) time-stable pattern (i.e., temporal
92 mean, spatial forcing): the “static” factors such as soil and topography control the
93 pattern; (2) space-invariant temporal anomaly (temporal forcing): the “dynamic”
94 factors such as meteorological variables and vegetation change with time, and
95 therefore modify SWC in time, regardless of spatial locations; and (3) space-variant
96 temporal anomaly (interactions between spatial forcing and temporal forcing): this
97 term represents interactions between “static” and “dynamic” factors. For example,
98 SWC recharge introduced by a rainfall may be modified by topography through
99 runoff processes; SWC loss triggered by evapotranspiration may be regulated by
100 topography through solar radiation exposure.

101 | The “static” factors ~~can~~may be persistent in the space-variant temporal anomaly,
102 and their impacts on the space-variant temporal anomaly likely change with time.
103 Thus, we hypothesize that some underlying (i.e., time-invariant) spatial patterns exist
104 in the space-variant temporal anomaly, and their impacts can be modulated by a time
105 coefficient, both of which can be obtained by the EOF method (Fig. 1). If the
106 | hypothesis is true, the estimation of spatially distributed SWC utilizing the EOF
107 decomposition may outperform the one suggested by Perry and Niemann (2007). This
108 is because: (1) the spatial anomaly which was decomposed using the EOF in Perry

109 and Niemann (2007) lumped the time-stable pattern and space-variant temporal
110 anomaly together (Fig. 1); (2) the underlying spatial patterns in the spatial anomaly
111 may not fully capture both time-stable patterns and patterns in the space-variant
112 temporal anomaly due to the possible nonlinear relations between these two terms.

113 Therefore, the objectives were (1) to test the hypothesis that underlying spatial
114 patterns exist in the space-variant temporal anomaly at small watershed scales and (2)
115 to examine whether the decomposition of the space-variant temporal anomaly using
116 the EOF has any advantages over the decomposition of the spatial anomaly (Perry and
117 Niemann, 2007) for estimating spatially distributed SWC. Two steps were included in
118 the estimation of spatially distributed SWC. First, the spatial mean SWC was upscaled
119 from the SWC measurement at the most time-stable location using ~~the~~ time stability
120 analysis. ~~Then Following this, the~~ spatially distributed SWC was downscaled from the
121 estimated spatial mean SWC. For ~~this-the~~ purpose of this study, spatiotemporal SWC
122 datasets ~~from-at~~ depths of near surface (0–0.2 m) and root zone (0–1.0 m) from a
123 Canadian prairie landscape were used. Spatiotemporal SWC of samples taken 0–0.06
124 m from a hillslope (100 m) in the Chinese Loess Plateau and 0–0.15 m from the
125 GENCAI network (~250 km²) in Italy were also used to further demonstrate
126 conditions under which the decomposition of the spatial anomaly was beneficial to the
127 estimation of spatially distributed SWC.

Formatted: English (Canada)

128 2. Materials and methods

129 2.1 Study area and data collection

130 ~~The~~is study ~~area was conducted in the Canadian prairie pothole region at~~ ~~is located~~
131 ~~in~~ St. Denis National Wildlife Area (52°12' N, 106°50' W) ~~and has~~with an area of 3.6
132 km² ~~in the Canadian prairies~~. This area has a humid continental climate (Peel et al.,
133 2007), ~~and had a mean annual air temperature of 1.9 °C and a mean annual~~
134 ~~precipitation of 402 mm during the study period (Fig. 2)~~. A variety of depressions,
135 knolls, and knobs result in a sequence of undulating slopes (Biswas et al., 2011). The
136 elevation varies from 554.8 to 557.5 m. The soils are dominated by clay loam
137 textured Mollisols (Soil Survey Staff, 2010) and covered by mixed grass, i.e., smooth
138 brome grass (*Bromus inermis*) and alfalfa (*Medicago sativa* L.). ~~The~~ ~~N~~near surface
139 soil porosity ranges from 38% (knolls) to 70% (depressions). Calcium carbonates
140 (CaCO₃) derived mostly from fragments of limestone rocks are common in the
141 Canadian Prairies. The CaCO₃ is dissolved by the slightly acidic rainwater moving
142 through the upper horizons and deposited to lower horizons. The heterogeneous
143 amount of infiltrated water resulted in a varying depth of CaCO₃ layer ranging from
144 almost 0 m in the knolls to 2.1 m in the depressions. A 576 m long sampling transect
145 ~~576 m long~~ with 128 sampling locations spaced at 4.5 m intervals was established
146 over several rounded knolls and depressions. At each location, a time domain
147 reflectometry probe was used to measure SWC of the near surface soil (0–0.2 m), and
148 a neutron probe was used to collect SWC measurements at 0.2 m intervals between a
149 depth of 0.2 and 1.0 m. The SWC was measured on a volumetric basis and expressed

Formatted: Subscript

150 as a percentage (%) volume of water per unit soil volume. The SWC of the root zone
151 was calculated by averaging the SWC of 0–0.2, 0.2–0.4, 0.4–0.6, 0.6–0.8, and 0.8–1.0
152 m. Soil water content was measured on 23 dates from ~~17~~ July 17, 2007 to ~~29~~
153 September 29, 2011. The SWC dataset was collected in all seasons except winter, and
154 accurately portrays the variations in soil water conditions in the study area. In addition
155 to the SWC dataset, the soil, vegetative, and topographical properties were obtained at
156 each sampling location ~~(Biswas et al., 2012).~~ These properties included soil particle
157 components (clay, silt, and sand contents), bulk density, soil organic carbon (SOC)
158 content for the surface layer, A horizon depth, C horizon depth, depth to the CaCO₃
159 layer, leaf area index, elevation, cos(aspect), slope, curvature, gradient, upslope length,
160 solar radiation, specific contributing area, convergence index, wetness index, and flow
161 connectivity. Detailed information on the measurements can be found in Biswas et al.
162 ~~(2012) These properties were used to relate time-stable patterns and underlying spatial~~
163 ~~patterns of space-variant temporal anomaly to environmental factors.~~

164 2.2 Statistical models for decomposing soil water content

165 Spatiotemporal SWC at small watershed scales was decomposed into three
166 components: time-stable pattern, space-invariant temporal anomaly, and space-variant
167 temporal anomaly. For estimation of spatially distributed SWC, further decomposition
168 of space-variant temporal anomaly was conducted using the EOF method. In order to
169 show advantages of tThis model was compared to overthe one that developed by
170 Perry and Niemann (2007), decomposed SWC was also decomposed into spatial mean
171 and spatial anomaly, with the latter being further decomposed using the EOF method

Formatted: List Paragraph, Indent:
First line: 0 ch

(Perry and Niemann, 2007). Both the space-variant temporal anomaly and spatial anomaly were decomposed using the EOF method. The two models are termed temporal anomaly (TA) model and spatial anomaly (SA) model, respectively. Please refer to Figure 1 displays for the differences of between the two models. Each component will be explained in detail later. The explanation of nomenclatures is listed in Table A1. Because we focus on estimating spatial distribution of SWC at any given time, only spatial variances of SWC were taken into account in this study. Therefore, the variance or covariance denotes the quantity in space without specifications.

2.2.1 The SA model

Perry and Niemann (2007) expressed SWC at location n and time t (S_m) as (Fig. 1):

$$S_m = S_{\hat{m}} + Z_m, \quad (1)$$

where $S_{\hat{m}}$ is the spatial mean SWC at time t (temporal forcing) and Z_m is the spatial anomaly of SWC (lumped spatial forcing and interactions). The subscript \hat{m} (\hat{t}) indicates a space (time) averaged quantity.

According to Perry and Niemann (2007), $S_{\hat{m}}$ can be estimated by remote sensing, water balance models, and in situ soil water measurement at a representative (or time-stable) location. The in situ soil water measurement method was selected because the representative location can be easily determined with prior SWC datasets.

By measuring SWC only at the most time-stable location (s) and future time t (S_{ts}),

$S_{\hat{m}}$ can be estimated using SWC at the most time-stable location s and time t , S_{ts} .

$S_{\hat{m}}$ in Eq. (1) was obtained from SWC at the most time-stable location s and time t , S_{ts} ,

using (Grayson and Western, 1998):

Formatted: Font color: Auto

Formatted: Font color: Auto

Formatted: Font: Not Italic

Formatted: English (Canada)

Formatted: Font: (Default) Times New Roman, 12 pt

Formatted: Font: (Default) Times New Roman, 12 pt

Formatted: Indent: First line: 1 ch

Field Code Changed

Formatted: Font: Not Italic

Field Code Changed

Field Code Changed

195

$$S_{\hat{m}} = \frac{S_{ts}}{1 + \delta_{ts}} \quad , \quad (2)$$

196

where ~~the the most time stable location~~s was identified using the time stability index of mean absolute bias error (Hu et al., 2010, 2012). The δ_{ts} is the temporal mean relative difference of SWC at the ~~most time stable location~~s, ~~which was~~ calculated with prior measurements.

197

198

199

200

201

202

203

204

205

206

207

208

209

210

211

212

213

Spatial anomaly (Z_m) can be reconstructed by the sum of the product of time-invariant spatial structures (EOFs) and temporally varying coefficients (ECs) using the EOF method ~~is decomposed into a series of time invariant spatial patterns (EOFs) (Perry and Niemann, 2007). The sum of products of the EOFs and the temporally varying (but spatially constant) coefficients (ECs) leads to the reconstructed original Z_m in a space time domain~~ (; Joshi and Mohanty, 2010; Vanderlinden et al., 2012). The ECs correspond to the eigenvectors of the matrix of spatial covariance of the Z_m , and the EOFs are obtained by projecting the Z_m onto the matrix ECs as: $EOFs = Z_m ECs$. The number of EOF (or EC) series equals the number of sampling dates. Each EOF series corresponds to one value at each location, and each EC series has one value at each measurement time. Each ~~The i -th~~ EOF is chosen to be orthogonal to ~~other~~ the first through $(i - 1)$ th EOFs, and the lower-order EOFs and ~~accounts~~ for as much variance as possible. The sum of variances of all EOFs equals the sum of variances of Z_m from all measurement times.

214

215

216

Usually, a substantial amount of variance can be explained by a small number of EOFs. Johnson and Wichern (2002) suggested the eigenvalue confidence limits method for selecting the number of EOFs. Once the number of significant EOFs at a

Formatted: Font: (Default) Times New Roman, 12 pt

Formatted: Font: (Default) Times New Roman, 12 pt

Field Code Changed

Formatted: Font: (Default) Times New Roman, 12 pt

Field Code Changed

Formatted: Font: (Default) Times New Roman, 12 pt

Field Code Changed

217 confidence level of 95% is selected, Z_m can be estimated as the sum of the product
 218 of significant EOFs and associated ECs as:

$$219 \quad Z_m = \sum \text{EOF}^{\text{sig}} \times (\text{EC}^{\text{sig}})^T, \quad (3)$$

220 where EOF^{sig} represents the significant EOFs of the Z_m obtained during model
 221 development, EC^{sig} is the associated temporally varying coefficient, and the
 222 superscript T represents matrix transpose. Following Perry and Niemann (2007), The
 223 the associated significant EC at time t , (EC_t) , can be estimated by the cosine
 224 relationship between EC and S_m developed using prior measurements (Perry and
 225 Niemann, 2007):

$$226 \quad \text{EC}_t = a + b \cos\left(\frac{2\pi}{c} S_m - d\right), \quad (4)$$

227 where a , b , c , and d are the fitted parameters using prior measurements and S_m is
 228 estimated from Eq. (2). By using the continuous function, EC_t can be estimated at
 229 any S_m values, which allows for the estimation of spatially distributed SWC at any
 230 soil water conditions.

231 2.2.2 The TA model

232 Mittelbach and Seneviratne (2012) decomposed the ~~variance of~~ S_m into a
 233 time-stable pattern (i.e., temporal mean) and a temporal anomaly component (Fig. 1):

$$234 \quad S_m = M_m + A_m, \quad (5)$$

235 where M_m is the time-stable pattern (spatial forcing), ~~which is~~ controlled by
 236 ~~temporally constant but spatially varying factors~~ “static” factors such as soil properties
 237 and topography; ~~and~~ A_m refers to the temporal anomaly (lumped temporal forcing
 238 and interactions). The variance of SWC, $(\sigma_m^2(S_m))$, is the sum of variance of the

Formatted: Font: (Default) Times New Roman, 12 pt

Formatted: Font: (Default) Times New Roman, 12 pt

Field Code Changed

Formatted: Font: (Default) Times New Roman, 12 pt

Field Code Changed

Formatted: English (Canada)

Field Code Changed

Field Code Changed

239 ~~$M_{\hat{m}}$~~ , ~~$M_{\hat{m}}$~~ ($\sigma_{\hat{n}}^2(M_{\hat{m}})$), ~~the~~ variance of ~~the~~ ~~A_m~~ ($\sigma_{\hat{n}}^2(A_m)$), and two times of
240 covariance between $M_{\hat{m}}$ and ~~A_m~~ ($2\text{cov}(M_{\hat{m}}, A_m)$), which can be expressed
241 as:

$$242 \quad \sigma_{\hat{n}}^2(S_m) = \sigma_{\hat{n}}^2(M_{\hat{m}}) + 2\text{cov}(M_{\hat{m}}, A_m) + \sigma_{\hat{n}}^2(A_m). \quad (6)$$

243 Because ~~the~~ A_m in Mittelbach and Seneviratne (2012) is a lumped term, it can be
244 further decomposed into space-invariant temporal anomaly (~~A_m~~ , ~~i.e.~~, (temporal
245 forcing) and space-variant temporal anomaly (R_m , ~~i.e.~~, (interactions) ~~as~~
246 (Vanderlinden et al., 2012) ~~suggested~~. At a watershed scale, ~~the~~ A_m is controlled
247 by ~~spatially constant but~~ temporally varying factors such as meteorological variables
248 and vegetation (~~vegetation usually has greater variations over time than over space at~~
249 ~~small watershed scales~~). Positive and negative A_m correspond to relatively wet and
250 dry periods, respectively. The R_m refers to the redistribution of A_m among
251 different locations due to the interactions between spatial forcing and temporal
252 forcing. For example, soil and topography regulate how much rainfall enters soil and
253 how much water runs off or runs on at a location, ~~resulting in spatial variability in~~
254 ~~temporal anomaly~~. This, in turn, dictates vegetation growth in a water-limited
255 environment. Therefore, S_m can ~~also~~ be expressed as (Fig. 1):

$$256 \quad S_m = M_{\hat{m}} + A_m + R_m. \quad (7)$$

257 The temporal trends of A_m in Eq. (7) and S_m in Eq. (1) are the same, as both
258 represent temporal forcing. Because ~~the~~ A_m is space-invariant and orthogonal to ~~the~~

259 $M_{\hat{m}}$ and R_m in a space, $\sigma_{\hat{n}}^2(S_m)$ in Eq. (6) can also be written as:

$$260 \quad \sigma_{\hat{n}}^2(S_m) = \sigma_{\hat{n}}^2(M_{\hat{m}}) + 2\text{cov}(M_{\hat{m}}, R_m) + \sigma_{\hat{n}}^2(R_m), \quad (8)$$

261 where $\text{cov}(M_{\hat{m}}, R_m)$ is the covariance between the $M_{\hat{m}}$ and R_m , and $\sigma_{\hat{n}}^2(R_m)$ is
 262 the variance of the R_m . Apparently, $2\text{cov}(M_{\hat{m}}, R_m)$ equals $2\text{cov}(M_{\hat{m}}, A_m)$, and
 263 $\sigma_{\hat{n}}^2(R_m)$ equals $\sigma_{\hat{n}}^2(A_m)$. The percent (%) contributions of $\sigma_{\hat{n}}^2(M_{\hat{m}})$, $2\text{cov}(M_{\hat{m}}, R_m)$, and $\sigma_{\hat{n}}^2(R_m)$ to the $\sigma_{\hat{n}}^2(S_m)$ are calculated. The $\text{cov}(M_{\hat{m}}, R_m)$
 264 can be negative at some conditions, for example, when the depressions correspond to
 265 greater $M_{\hat{m}}$ and more negative R_m values in the discharge periods. This resulted
 266 in percentage contributions of $\sigma_{\hat{n}}^2(M_{\hat{m}})$ and $\sigma_{\hat{n}}^2(R_m)$ > 100% and percentage
 267 contributions of $2\text{cov}(M_{\hat{m}}, R_m)$ < 0% (Mittelbach and Seneviratne, 2012; Brocca et
 268 al., 2014; Rötzer et al., 2015). If R_m is zero at any time or location, there are no
 269 interactions between spatial forcing and temporal forcing, $\sigma_{\hat{n}}^2(S_m)$ and the spatial
 270 trends of SWC are consistent over time. Therefore, R_m is directly responsible for a
 271 temporal change in the spatial variability of SWC.

273 If some underlying spatial patterns exist in R_m , R_m can be reconstructed by the
 274 sum of the product of time-invariant spatial structures (EOFs) and time-dependent
 275 coefficients (ECs) using the EOF method. Note that the number of EOF (or EC) series
 276 also equals the number of sampling dates.

277 For estimation of spatially distributed SWC, R_m is estimated by the same method
 278 as Z_m using Eq. (3). The $M_{\hat{m}}$ is estimated with prior measurements by:

$$M_{\hat{m}} = \frac{1}{m} \sum_{j=1}^m S_m, \quad (9)$$

280 where m is the number of previous measurement times, and $A_{\hat{m}}$ is estimated by:

$$A_{\hat{m}} = S_{\hat{m}} - M_{\hat{m}}, \quad (10)$$

282 where $M_{\hat{m}}$ is the spatial mean of $M_{\hat{m}}$, and $S_{\hat{m}}$ is estimated from SWC

Field Code Changed

Field Code Changed

Field Code Changed

Field Code Changed

Field Code Changed

Field Code Changed

Field Code Changed

Field Code Changed

Field Code Changed

Field Code Changed

283 measurements at the most time-stable location using Eq. (2).

284 ~~These properties were used to relate time stable patterns and underlying spatial~~
285 ~~patterns of space variant temporal anomaly to environmental factors.~~ The Pearson
286 correlation coefficient (R) is used to explore the linear relationships between various
287 spatial components in the two models (i.e., EOF1 of the Z_m in the SA model, $M_{\hat{m}}$,
288 and EOF1 of the R_m in the TA model) and environmental factors (i.e., soil,
289 vegetative, and topographical properties). The multiple stepwise regressions are
290 conducted to determine the percentage of variations in the spatial components which
291 the controlling factors explain.

Formatted: Normal, Don't adjust right indent when grid is defined, Don't adjust space between Latin and Asian text, Don't adjust space between Asian text and numbers

Formatted: Font: Italic

Field Code Changed

Field Code Changed

Formatted: Font: (Default) Times New Roman, 12 pt

Field Code Changed

292

Formatted: Indent: First line: 1 ch, Don't adjust right indent when grid is defined, Don't adjust space between Latin and Asian text, Don't adjust space between Asian text and numbers

293 2.3 Validation and performance parameter

294 The TA model is more complicated than the SA model. In order to evaluate the two
295 models for parsimony, AICc values are calculated (Burnham and Anderson, 2002) as:

$$296 \text{AICc} = 2k + n \ln(\text{RSS} / n) + 2k(k + 1) / (n - k - 1), \quad (11)$$

297 where k is the number of parameters, n is the sample size, and RSS is the residual sum
298 of squares.

299 Both cross validation and external validation are used to estimate SWC distribution
300 with both models. For the C_{cross} validation ~~is used to estimate SWC distribution~~
301 along the transect with both models. A, an iterative removal of 1 of the 23 dates is
302 made for model development, and the SWC along the transect corresponding to the
303 removed date is estimated iteratively. For the external validation, SWC from 14 dates
304 of the first two years (from July 17, 2007 to May 27, 2009) is used for model

305 development, and the SWC distribution of 9 dates in the second two years (from July
306 21, 2009 to September 29, 2011) is estimated.

307
308 The Nash-Sutcliffe coefficient of efficiency (NSCE) is used to evaluate the quality
309 of estimation of spatially distributed SWC, which is expressed as:

310
$$\text{NSCE} = 1 - \frac{\sigma_{\varepsilon}^2}{\sigma_{\text{measure}}^2}, \quad (12)$$

311 where $\sigma_{\text{measure}}^2$ is the variance of measured SWC, and σ_{ε}^2 is the mean squared

312 estimation error. A larger NSCE value implies a better quality of estimation. A paired

313 samples T-test is used to test whether the NSCE values between the TA model and the

314 SA model are statistically significant at $P < 0.05$.

- Formatted: Font color: Auto, Not Highlight
- Formatted: Font color: Auto, Not Highlight
- Formatted: Font color: Auto, Not Highlight
- Formatted: Font color: Auto
- Formatted: Font color: Auto, Not Highlight
- Formatted: Font color: Auto
- Formatted: Font color: Auto, Not Highlight
- Formatted: Font color: Auto, Not Highlight
- Formatted: Font color: Auto, Not Highlight
- Formatted: Font color: Auto, Not Highlight
- Formatted: Font color: Auto, Not Highlight
- Formatted: Font color: Auto

accuracy of the S_{in} . Because the same S_{in} values are used for the two models,
the relative performance of the two models is related to the goodness of fit of Eq.
(4).

- Formatted: Font: Not Bold
- Formatted: Font: Not Bold
- Formatted: Font: Not Bold
- Field Code Changed
- Formatted: Font: Not Bold
- Field Code Changed
- Formatted: Font: Not Bold
- Formatted: Font color: Auto

3. Results

4 Results

- Formatted: Indent: Left: 0.63 cm, No bullets or numbering

4.1.3.1 Components of SWC and their controls

3.1.1 Spatial mean (S_{in}) and spatial anomaly (Z_m)

- Formatted: Font: (Default) Times New Roman

- Formatted: Space Before: 12 pt

The values of spatial mean (S_{in}) in the SA model varied with the seasons (Fig. 2a3a). In the spring, such as 2-May 2, 2008 and 20-April -20, 2009, snowmelt infiltration resulted in relatively great S_{in} values. In the summer, however, even one month after large rainfall events (such as on 19-July 19, 2008 and 21-June -21, 2009), the high evapotranspiration by fast-growing vegetation resulted in small S_{in} values. The values of S_{in} also varied between inter-annual meteorological conditions. In 2008, there was less precipitation and higher air temperature than in 2010 (Fig. 2). As a result, S_{in} was relatively smaller in 2008 than in 2010.

The spatial patterns of spatial anomaly (Z_m) were similar to those of original SWC pattern. Two individual dates that had contrasting soil water conditions are shown in Fig. 2b. The values of Z_m in a wet periods (e.g., 13-May 13, 2011) were much greater than in a dry periods (e.g., 23-August 23, 2008) in depressions (e.g., at a

357 distance of 123 and 250 m); at other locations, however, the spatial anomaly was
358 slightly less in ~~a~~ wet periods than in ~~a~~ dry periods for both soil layers. Moreover, the
359 spatial anomaly in depressions ~~during the wet periods~~ ~~during wet periods~~ was much
360 greater in the near surface than in the root zone.

361 When SWCs of all 23 dates were used for model development, only EOF1 was
362 statistically significant (Fig. ~~3a4a~~), which accounted for 84.3% (0–0.2 m) and 86.5%
363 (0–1.0 m) of the variances in the Z_m . Correlation analysis indicated that the spatial
364 pattern of EOF1 in the Z_m was identical to the time-stable patterns (M_{in}) in the TA
365 model ($R=1.0$). The controls of EOF1 was therefore the same as those of M_{in} , and
366 will be discussed later. The relationship between associated EC1 and S_{in} can be
367 fitted well by the cosine function ($R^2=0.73$ at both the near surface and root zone) (Fig.
368 ~~3b4b~~).

369 **3.1.2 Time-stable pattern (M_{in}), space-invariant temporal anomaly (A_{in}), and** 370 **space-variant temporal anomaly (R_m)**

371 Figure ~~4-3b~~ displays the three components in the TA model. The first component
372 M_{in} fluctuated along the transect, with high values in depressions and low values on
373 knolls (~~Fig. 4a~~); ~~the~~ M_{in} also had greater spatial variability in the near surface
374 (variance =36.7%²) than in the root zone (variance=19.5%²). For both soil layers, ~~soil~~
375 ~~organic carbon content~~ (SOC), depth to the CaCO₃ layer, sand content, and wetness
376 index are the dominant factors of M_{in} ; they together explained 74.5% (near surface)
377 and 75.6% (root zone) of the variances in ~~the~~ M_{in} (Table 1). In addition, the
378 temporal trend of A_{in} (~~Fig. 4b~~) was the same as that of S_{in} in the SA model (Fig.

Formatted: Font: Italic

379 ~~2b3a~~); as both represent temporal forcing.

380 The R_m varied among landscape positions (Fig. 4e). At a sampling distance of
381 123 m (in a depression), R_m was negative in dry periods such as ~~23~~-August 23, 2008
382 and positive in wet periods such as ~~13~~-May 13, 2011. This was true for all depressions
383 for both the near surface and the root zone. Therefore, topographically lower positions
384 usually corresponded to more positive R_m during the wet periods and more negative
385 R_m during the dry periods. This implies that topographically lower locations gained
386 more water during recharge and lost more water during discharge due to the
387 interactions of spatial and temporal forcing. Furthermore, the absolute values of R_m
388 were generally greater in the near surface than the root zone, indicating a greater
389 space-variant temporal anomaly for shallower depths.

390 The SWC variances and associated components (Eq. 8) also varied with time (Fig.
391 5). Often, wetter conditions corresponded to greater $\sigma_n^2(S_m)$, as further indicated by
392 moderate correlation between $\sigma_n^2(S_m)$ and S_m (R^2 of 0.51 and 0.38 for the near
393 surface and the root zone, respectively). This was in agreement with others
394 (Gómez-Plaza et al., 2001; Martínez-Fernández and Ceballos, 2003; Hu et al., 2011).
395 Furthermore, there were greater $\sigma_n^2(S_m)$ values at near surface than in the root zone,
396 indicating greater variability of SWC in the near surface.

397 The time-invariant $\sigma_n^2(M_m)$ contributed to the $\sigma_n^2(S_m)$ with percentages
398 ranging from 25 to 795% for the near surface and from 40 to 174% for the root zone
399 (Fig. 5). The $\sigma_n^2(M_m)$ exceeded the $\sigma_n^2(S_m)$ mainly under dry conditions, such as

400 July–October in 2008 and 2009. This excess was offset by the $\sigma_n^2(S_m)$ and
401 $2\text{cov}(M_n, R_m)$, ~~with and~~ the latter contributing negatively to the $\sigma_n^2(S_m)$ with
402 mean percentages of -210% for the near surface and 17% for the root zone. In the dry
403 period, the negative contribution from $2\text{cov}(M_n, R_m)$ was up to 1327% for the near
404 surface and 122% for the root zone. These values are comparable to those in
405 Mittelbach and Seneviratne (2012) and Brocca et al. (2014).

406 The $\sigma_n^2(R_m)$ contributed less than other components (Fig. 5). The percentages of
407 $\sigma_n^2(R_m)$ ranged from 11 to 632% (arithmetic average of 118%) for the near surface
408 and from 6 to 48% (arithmetic average of 19%) for the root zone; $\sigma_n^2(R_m)$ tended to
409 contribute more in drier periods. This indicates that the space-variant temporal
410 anomaly cannot be ignored, particularly in dry conditions. Furthermore, the
411 contribution of $\sigma_n^2(R_m)$ was greater in the near surface than in the root zone,
412 confirming stronger temporal dynamics of soil water at the near surface. Compared
413 with larger scale studies (Mittelbach and Seneviratne, 2012; Brocca et al., 2014),
414 $\sigma_n^2(R_m)$ of the near surface ~~in this study~~ contributed more to $\sigma_n^2(S_m)$, with a mean
415 percentage contribution of 118%, versus 9–68% in the other, larger scale studies
416 (~~Mittelbach and Seneviratne, 2012; Brocca et al., 2014~~). This indicates that
417 interactions between spatial and temporal forcing were stronger, resulting in relatively
418 more intensive temporal dynamics of soil water in our study area than at larger scales.

419 Three significant EOFs of R_m for both soil layers were identified when SWC of
420 all 23 dates were used for model development. The first three EOFs explained 61.1,
421 13.4, and 8.1% respectively, of the total R_m variance for the near surface, and 44.3,

422 | 20.2, and 12.4%, respectively, of the total R_m variance ~~for~~in the root zone.
423 | Therefore, our hypothesis that underlying spatial patterns exist in the R_m was
424 | accepted. Due to the negligible contribution of EOF2 and EOF3 to the estimation of
425 | spatially distributed SWC, only EOF1 is shown in Fig. 6a. The associated EC1
426 | changed with soil water conditions (S_m) (Fig. 6b). When SWC was close to average
427 | levels, the EC1 was close to 0, resulting in negligible R_m . This was in accordance
428 | with Mittelbach and Seneviratne (2012) and Brocca et al. (2014), who showed that the
429 | spatial variance of the temporal anomaly was the smallest when water contents were
430 | close to average levels. The cosine function (Eq. ~~114~~) explained a large amount of the
431 | variances in EC1 for both soil layers ($R^2=0.76$ at the near surface and 0.88 in the root
432 | zone).

433 | The contribution of EOF1 to the space-variant temporal anomaly can be examined
434 | through the product of the EOF1 and the associated EC1. The EC1 values tended to
435 | be positive during wet periods and negative during dry periods (Fig. 6b); more
436 | positive EOF1 values were usually observed at locations with greater $M_{\hat{m}}$ values
437 | (Figs. ~~4a-3b~~ and 6a). Therefore, the product of EOF1 and EC1 led to greater temporal
438 | SWC dynamics at wetter locations of both layers in both the wet and dry periods.

439 | Depth to the CaCO_3 layer and SOC had significant, positive correlations with
440 | EOF1 for both soil layers (R ranging from 0.76 to 0.88; Table 1). They jointly
441 | accounted for 81.6% (near surface) and 81.0% (root zone) of the variances in EOF1.
442 | This implies that locations with a greater depth to the CaCO_3 layer and SOC, which
443 | correspond to wetter locations such as depressions, usually have greater temporal

444 SWC dynamics during both wet and dry periods.

445 **4.23.2 Estimation of spatially distributed SWC**

446 When all 23 datasets were used and only EOF1 was considered, the TA model had
447 an AICc value of 4093 for the near surface and 562 for the root zone, while the
448 corresponding values for the SA model were 6370 and 3460. This indicated that even
449 when penalty to complexity was given, the TA model was better than the SA model.
450 The two models in terms of ~~estimation of~~ spatially distributed SWC estimation are
451 compared below.

452 **3.2.1 The TA model**

453 The R_m terms and associated EOFs differed slightly with each validation. The
454 number of significant EOFs varied between one (accounting for 60% of the total cases)
455 and three for both soil layers. A ~~p~~Paired ~~Samples-samples~~ T-test indicated that more
456 EOFs did not result in a significant increase of NSCE in the estimation of spatially
457 distributed SWC for both validation methods, because AICc values increased greatly
458 with the increasing number of parameters resulting from more EOFs (data not shown).
459 This indicates that higher-order EOFs, even if they are statistically significant, are
460 negligible for SWC prediction. Therefore, SWC distribution was estimated with
461 EOF1 only.

462 Estimated SWCs generally approximated those measured at different soil water
463 conditions during the cross validation (Fig. 7). However, on ~~27~~October 27, 2009,
464 there were unsatisfactory estimates at the 100–140 and 220–225 m locations near the
465 surface. Unsatisfactory NSCE values of -4.05, -1.83, and -3.81 were obtained in the

466 near surface in only three of the 23 dates, which were all in the fall (~~22~~–October 22,
467 2008, ~~27~~–August 27, 2009, and ~~27~~–October 27, 2009, respectively). The poor
468 performance obtained with the TA model on those dates was a result of overestimation
469 in depressions, where strong evapotranspiration and deep drainage resulted in a much
470 lower SWC than in the spring. These dates also corresponded to a high percentage of
471 contribution of $\sigma_n^2(R_m)$ to the $\sigma_n^2(S_m)$ (203—439%). For August 23 and
472 September 17 in 2008, which were in dry periods, $\sigma_n^2(R_m)$ of the near surface also
473 contributed highly to the $\sigma_n^2(S_m)$ (580 and 630%). Because a fair amount of
474 $\sigma_n^2(R_m)$ was accounted for with the TA model, the TA model performed
475 satisfactorily (NSCE of 0.43 and 0.60). ~~For~~

476 ~~For~~ the remaining 20 dates, the resulting NSCE value ranged from 0.38 to 0.90 in
477 the near surface and from 0.65 to 0.96 in the root zone (Fig. 8). This suggests that the
478 TA model was generally satisfactory, with better performance in the root zone than in
479 the near surface.

480 During the external validation, the TA model resulted in SWC estimations with
481 NSCE values ranging from 0.61 to 0.85 near the surface and from 0.32 to 0.92 in the
482 root zone, with exception of two days (August 27, 2009 and October 27, 2009 with
483 NSCE values of -2.63 and -5.12, respectively) at 0–0.2 m (Fig. 8). This suggested that
484 the TA model performed well in estimating spatially distributed SWC patterns except
485 on August 27, 2009 and October 27, 2009 at 0–0.2 m. The estimation in the root zone
486 was also generally better than in the near surface.

487

488 3.2.2 Comparison with the SA model

489 One significant EOF of Z_m was identified ~~in each validation~~ for both soil layers,
490 irrespective of the validation method. The SA model with only EOF1 produced
491 reasonable SWC estimations for both validations in all dates in the root zone and in
492 every date except five dates (~~23~~-August 23, 2008, ~~17~~-September 17, 2008, ~~22~~-October
493 22, 2008, ~~27~~-August 27, 2009, and ~~27~~-October 27, 2009) in the near surface (Fig. 8).
494 Similarly, when more EOFs were included, NSCE values did not increase
495 significantly (data not shown) and consequently, estimation of spatially distributed
496 SWC was not improved. This was because EOF2 and EOF3 together explained a very
497 limited (<10%) amount of variability of Z_m and thus had low predictive power in
498 terms of variance.

499 The difference in NSCE values between the TA and SA models for both validations
500 are presented in Fig. 9. Generally, the difference decreased as $A_{\hat{m}}$ increased, and
501 then slightly increased with a further increase in $A_{\hat{m}}$. A paired samples T-test
502 indicated that the NSCE values of the TA model were significantly ($P<0.05$) greater
503 than those of the SA model for both soil layers, irrespective of validation methods.
504 ~~The-This indicates that the~~ TA model outperformed the SA model, ~~as indicated by a~~
505 ~~positive NSCE difference~~, particularly in dry conditions. This was because when the
506 soil was dry, there was a high contribution of $\sigma_n^2(R_m)$, and thus strong variability in
507 the space-variant temporal anomaly.

508 **3.3 Further application at other two sites with different scales**

509 **3.3.1 A hillslope in the Chinese Loess Plateau**

Formatted: Font: Bold

Formatted: Normal, No bullets or numbering

Formatted: Font: Bold

510 Along a hillslope of 100 m in length in the Chinese Loess Plateau, SWC of 0–0.06
511 m was measured 136 times from June 25, 2007 to August 30, 2008 by a Delta-T
512 Devices Theta probe (ML2x) at 51 locations (Hu et al., 2011). The hillslope was
513 covered by *Stipa bungeana* Trin. and *Medicago sativa* L. in sandy loam and silt loam
514 soils. On average, the $\sigma_n^2(M_m)$, $\sigma_n^2(R_m)$, and $2\text{cov}(M_m, R_m)$ contributed 53, 74
515 and -27% to the $\sigma_n^2(S_m)$, indicating that both time-stable pattern and temporal
516 anomalies were the main contributors to the $\sigma_n^2(S_m)$. The EOF analysis showed that
517 only the EOF1 was statistically significant for both the R_m and Z_m , and the EOF1
518 explained 23% and 47% of the total variances of R_m and Z_m , respectively. This
519 illustrated that underlying spatial patterns exist in the R_m on the hillslope. Cross
520 validation was used to estimate the spatially distributed SWC along the hillslope. The
521 results showed that the NSCE varied from -4.25 to 0.83 (TA model) and from -4.30 to
522 0.81 (SA model), with a mean value of 0.25 and 0.18, respectively. A paired samples
523 T-test showed that the NSCE values for the TA model were significantly ($P<0.05$)
524 greater than those for the SA model, indicating that the TA model outperformed the
525 SA model. As Fig. 10a shows, the outperformance was greater when SWC deviated
526 from intermediate conditions, especially for dry conditions, which was similar to the
527 Canadian site.

- Formatted: Font color: Auto
- Field Code Changed
- Formatted: Font color: Auto
- Field Code Changed
- Field Code Changed
- Field Code Changed
- Field Code Changed
- Field Code Changed
- Field Code Changed
- Field Code Changed
- Field Code Changed

528 **3.3.2 The GENCAI network in Italy**

- Formatted: First line: 0 ch
- Formatted: Normal, Indent: First line: 0 ch

529 In the GENCAI network (~250 km²) in Italy, SWC of 0–0.15 m was measured by a
530 TDR probe at 46 locations, 34 times from February to December in 2009 (Brocca et
531 al., 2012, 2013). The GENCAI area was dominated by grassland with a flat

532 topography, in silty clay soils. The $\sigma_{\hat{n}}^2(M_{\hat{n}})$, $\sigma_{\hat{n}}^2(R_m)$, and $2\text{cov}(M_{\hat{n}}, R_m)$
 533 contributed 38, 68, and -7% to the $\sigma_{\hat{n}}^2(S_m)$ (Brocca et al., 2014), indicating the
 534 dominant contribution of temporal anomalies on SWC variability. The first three
 535 EOFs of the R_m explained 19, 16, and 8% of the total $\sigma_{\hat{n}}^2(R_m)$, and no EOFs were
 536 statistically significant, indicating that no underlying spatial patterns exist in the R_m .
 537 The EOF1 of the Z_m was significant and accounted for 37% of the variances in the
 538 Z_m . Although the EOF1 of the R_m was not significant, it was considered in the TA
 539 model for estimating spatially distributed SWC. The cross validation indicates that the
 540 NSCE varied from -0.79 to 0.50 (TA model) and from -0.87 to 0.56 (SA model), with
 541 mean values of 0.09 and 0.08, respectively. The SWC estimation based on these two
 542 models was not satisfactory except for a few days. As Fig. 10b shows, the differences
 543 in NSCE values between the two models were scattered around 0. A paired samples
 544 T-test showed that the NSCE values between the TA model and the SA model were
 545 not significant ($P < 0.05$), indicating no differences in estimating spatially distributed
 546 SWC between these two models.

547 **5.4 Discussion**

548 **4.1 Controls of the $M_{\hat{n}}$ and R_m**
 549 ~~Space-variant temporal anomaly.~~ The R_m played an important role in the temporal
 550 change ~~of~~ in spatial patterns ~~in~~ of the SWC. The underlying spatial patterns and
 551 physical meaning in the R_m were examined in our study for the first time.
 552 Although three significant EOFs ~~existed in the~~ of the R_m ~~existed in~~ for some cases,

Field Code Changed
 Field Code Changed
 Field Code Changed
 Field Code Changed

Field Code Changed
 Field Code Changed
 Field Code Changed

Field Code Changed

Field Code Changed
 Field Code Changed

Field Code Changed
 Formatted: Font color: Text 1
 Formatted: Heading 2, Indent: Left: 0 cm, Hanging: 0.63 cm, First line: 0 ch, Outline numbered + Level: 2 + Numbering Style: 1, 2, 3, ... + Start at: 1 + Alignment: Left + Aligned at: 0.63 cm + Indent at: 1.26 cm
 Formatted: Font color: Text 1
 Formatted: Font color: Text 1
 Field Code Changed
 Formatted: Font color: Text 1

553 ~~only EOF1 was needed for the estimation of spatially distributed SWC with the TA~~
554 ~~model.~~ only EOF1 rather than higher-order EOFs of the R_m should be considered for
555 the spatially distributed SWC estimation. –Among many factors influencing the
556 EOF1 of the R_m , depth to the CaCO₃ layer followed by the SOC, were the most
557 important factors. Depressions have deeper CaCO₃ layers than knolls, and the shallow
558 CaCO₃ layer on knolls limited water infiltration during rainfall or snowmelt, resulting
559 in less water recharge on knolls than in depressions. The depth to CaCO₃ layer and
560 SOC were negatively correlated with elevation ($R=-0.54$, $P<0.01$). Therefore, the
561 influence of depth to CaCO₃ layer and SOC partially reflected the role of topography
562 in driving snowmelt runoff along slopes in the spring, which contributes to increasing
563 water recharge in depressions. Locations with greater SOC usually corresponded to
564 vegetation with a larger leaf area index ($R=0.23$, $P<0.05$), which would also result in
565 higher evapotranspiration and more water loss during discharge periods.

Field Code Changed

566 As Table 1 shows, both the depth to the CaCO₃ layer and SOC controlled the M_{tn}
567 ~~time-stable patterns of SWC.~~ This was because deeper CaCO₃ layers and higher SOC
568 were observed in depressions where soils were usually wetter in most of the year
569 because of the snowmelt runoff in the spring and rainfall runoff in the summer and
570 autumn (van der Kamp et al., 2003). Therefore, the roles of soil and topography were
571 two-fold: On one hand, they were highly correlated with the time-stable patterns and
572 thus the time stability of SWC (Gómez-Plaza et al., 2000; Mohanty and Skaggs, 2001;
573 Grant et al., 2004); On the other hand, they soil and topography, interplaying with
574 temporal forcing, triggered local-specific soil water change and destroyed time

Field Code Changed

575 stability of SWC. Their roles in protecting time stability persisted, but their roles in
576 destroying time stability varied with time. Greater $\sigma_n^2(R_m)$ implies greater
577 contribution of these factors in soil water dynamics, resulting in less time stability of
578 SWC.

579 4.2 Model performance for spatially distributed SWC estimation

Formatted: Heading 2, Indent: Left: 0 cm, Hanging: 0.63 cm, First line: 0 ch, Outline numbered + Level: 2 + Numbering Style: 1, 2, 3, ... + Start at: 1 + Alignment: Left + Aligned at: 0.63 cm + Indent at: 1.26 cm

Formatted: Font color: Text 1

Formatted: Font color: Text 1

Field Code Changed

Field Code Changed

Field Code Changed

580 The outperformance of the TA model for estimating spatial SWC at the Canadian
581 site and Chinese site can be partly explained by the high contribution percentages
582 (average of 19–118%) of the $\sigma_n^2(R_m)$ to the total variance. When SWC is close to
583 average levels, R_m is also close to zero, resulting in negligible variance contribution
584 from R_m to the total variance. In this case, the soil water patterns are stable, the SA

585 model performs well, and there will be little differences between these two models.

586 As is well known, the spatial patterns in soil water content are inherently time
587 unstable. For example, when evapotranspiration becomes the dominant process at the
588 small watershed scale, more water will be lost in depressions due to the denser
589 vegetation than on knolls (Millar, 1971; Biswas et al., 2012), effectively diminishing
590 the spatial patterns and increasing temporal instability. In this case, the $\sigma_n^2(R_m)$

Field Code Changed

591 contributes more to the total variance (e.g., high up to 632%) and the TA model may
592 outperform the SA model. This explained why the outperformance of the TA model
593 was more obvious in the dry conditions. For the GENCAI network in Italy, although
594 the $\sigma_n^2(R_m)$ contributed 68% of the total variance, the performance of the TA model

Field Code Changed

595 was identical to the SA model. This was because there were no underlying spatial
596 patterns in the R_m . Similarly, because the first underlying spatial pattern (i.e., EOF1)

Field Code Changed

597 explained greater percentages of the $\sigma_a^2(R_m)$ at the Canadian site (44–61%) than the
598 Chinese site (23%), the outperformance of the TA model over the SA model was more
599 obvious at the former site (Fig. 9 and 10a). Therefore, the TA model is advantageous
600 only if the contribution of $\sigma_a^2(R_m)$ to the total variance is substantial and underlying
601 spatial patterns exist in the R_m .

Field Code Changed

Field Code Changed

Field Code Changed

Field Code Changed

602 The existence of underlying spatial patterns in the R_m is related to the controlling
603 factors, which may be scale-specific.

604 ~~The control of R_m may be scale specific, which can consequently affect the~~
605 ~~performance of the TA model. At a basin scale (31,500 km²), Mittelbach and~~
606 ~~Seneviratne (2012) attributed the “static” factors such as soil texture and topography~~
607 ~~to time-stable spatial patterns, and meteorological conditions to temporal anomaly~~
608 ~~(lumped A_m and R_m).~~ At small scales, “static” factors such as the depth to the
609 CaCO₃ layer and SOC at the Canadian site may affect not only the time-stable
610 patterns but also the R_m . The persistent influence of “static” factors on the R_m
611 resulted in significant underlying spatial patterns in the R_m . Thus, the TA model

Formatted: Font color: Text 1, Not Highlight

612 outperformed really well the SA model at the small scales, as demonstrated above. The
613 control of R_m may be scale specific, which can consequently affect the performance
614 of the TA model. At large scales such as the basin scale or greater, time-stable patterns
615 may be controlled by, in addition to soil and topography (Mittelbach and Seneviratne,
616 2012), the climate gradient (Sherratt and Wheater, 1984); at those scales, R_m is
617 more likely to be controlled by the meteorological anomaly (i.e., spatially random
618 variation) (Walsh and Mostek, 1980), and the effects of soil and topography may be

619 reduced. Consequently, spatial patterns in the R_m may be weakened and the TA
620 model may have no advantages over the SA model ~~at those large scales such as for the~~
621 Italian site.

622
623 ~~The different performance between the TA model and the SA model at the small~~
624 ~~watershed scales may be associated with the way EOF decomposition is performed. In~~
625 ~~the SA model, EOF decomposition is performed on lumped time-stable patterns M_{in}~~
626 ~~and space-variant temporal anomaly R_m (Perry and Niemann, 2007). In the TA~~
627 ~~model, however, EOF decomposition was made only on R_m . In theory, the two~~
628 ~~models will be identical if M_{in} and underlying spatial patterns (EOF1) of R_m are~~
629 ~~perfectly correlated. In the TA model, The M_{in} and the underlying spatial patterns~~
630 (EOF1) in the R_m were controlled by the same spatial forcing (e.g., depth to CaCO₃
631 layer and SOC) at the Canadian site (Table 1), and they were correlated with an R^2 of
632 0.83 for the near surface and 0.42 for the root zone. Although the relationships
633 between M_{in} and R_m were strong, they were not strictly linear, suggesting that
634 M_{in} and R_m were affected differently by these factors. Therefore, Because of a the
635 nonlinear relationship between them, lumping M_{in} and R_m together, partially
636 contributed to the outperformance of as in the SA-TA model, would weaken the model
637 performance as compared to over the TA-SA model.

638 ~~From this aspect, the greater deviation from a linear relationship between M_{in}~~
639 ~~and EOF1 of R_m , lead to a greater outperformance of the TA model over the SA~~
640 ~~model. The relationship between the S_{in} and EC1 was better fitted by the cosine~~

Field Code Changed

641 function in the TA model than the SA model (Figs. 4b and 6b), with R_x^2 of 0.76 versus
642 0.73 in the near surface and 0.88 versus 0.73 in the root zone. The reduced scatter in
643 the S_{in} and EC1 relationship for the TA model may also partly explain the
644 outperformance of the TA model over the SA model.

Formatted: Font: Italic

Formatted: Superscript

Field Code Changed

645
646 ~~The degree of outperformance of the TA model over the SA model also depends on~~
647 ~~the relative R_m variance contribution to the total variance. Theoretically, the two~~
648 ~~models are also identical if variance of R_m is zero or there are no interactions~~
649 ~~between the spatial and temporal components (Fig. 1). Conversely, the greater~~
650 ~~variance of R_m , the stronger the outperformance of the TA model. Therefore, the~~
651 outperformance of the TA model over the SA model depends on counterbalance

652 between among the variance of R_m , the variance of R_m explained in the TA model,
653 and the linear correlation between the M_m and M_{in} and EOF1 of the R_m ; the variance
654 of R_m and the goodness of fit for the S_{in} and EC1 relationship. For example, the

Field Code Changed

Field Code Changed

Field Code Changed

655 variance of EOF1 in the R_m for the near surface (i.e., 264%²) was much greater than
656 that for the root zone (i.e., 43%²). However, M_m and underlying spatial patterns
657 (EOF1) in the R_m in the root zone deviated more from a linear relationship, and the
658 reduced scatter in the S_{in} and EC1 relationship in the TA model was more obviously
659 in the root zone than in the near surface. As a result, the outperformance of the TA
660 model was comparable between the near surface and root zone at the Canadian site
661 (Fig. 9).

Field Code Changed

662 ~~As demonstrated above, the R_m destroys the time-stable patterns, and a greater~~

663 value of $\sigma_n^2(R_m)$ indicates less time stable patterns. When SWC is close to average
664 levels, R_m is also close to zero, resulting in negligible variance contribution from
665 R_m to the total variance. In this case, the soil water patterns are stable, the SA model
666 performs well, and there will be little differences between these two models. As is
667 well known, the spatial patterns in soil water contents are inherently time unstable.
668 For example, when evapotranspiration becomes the dominant process at the small
669 watershed scale, more water will be lost in depressions due to the denser vegetation
670 than on knolls (Millar, 1971; Biswas et al., 2012), effectively diminishing the spatial
671 patterns and increasing temporal instability. In this case, the TA model may
672 outperform the SA model. Therefore, the degree of outperformance of the TA model
673 over the SA model depends on the amount of variances in the R_m in addition to the
674 degree of nonlinearity between the time stable pattern $M_{\hat{m}}$ and underlying spatial
675 patterns in the R_m . In the real world, the relations between the $M_{\hat{m}}$ and underlying
676 spatial patterns in the R_m may rarely be perfectly linear. Therefore, when underlying
677 spatial patterns exist in the R_m and the R_m has substantial variances, the TA model
678 is preferable to the SA model for the estimation of spatially distributed SWC. Because
679 the TA model was not worse than the SA model for the whole range of SWC, the TA
680 model is suggested for the estimation of spatially distributed SWC at different soil
681 water conditions. _

682 Previous studies on SWC decomposition mainly focus on near surface layers
683 (Jawson and Niemann, 2007; Perry and Niemann, 2007, 2008; Joshi and Mohanty,
684 2010; Korres et al., 2010; Busch et al., 2012). This study decomposed spatiotemporal

685 SWC using the TA model for both the near surface and the root zone. The results
686 showed that the estimation of spatially distributed SWC at small watershed scales was
687 improved by the TA method that considers the R_m . Because of the stronger time
688 stability of SWC in deeper soil layers (Biswas and Si, 2011), SWC evaluation in
689 thicker soil layers was more accurate than in shallow soil layers. This is particularly
690 important because SWC data for deeper soil layers in a watershed is more difficult to
691 collect than that of surface soil.

692 65 Conclusions

693 ~~A statistical model (The TA model)~~ was used to decompose spatiotemporal SWC
694 ~~from a small watershed scale in the Canadian prairies,~~ into time-stable patterns $M_{\hat{m}}$,
695 space-invariant temporal anomaly $A_{\hat{m}}$, and space-variant temporal anomaly R_m .

696 ~~This study indicated that The R_m was further decomposed by an EOF analysis to~~
697 ~~reveal the~~ underlying spatial patterns may exist in the R_m at small scales (e.g., small
698 watersheds and hillslope) but may not exist at large scales such as the GENCAI
699 network (~250 km²) in Italy. This was because the R_m at small scales was driven by

700 “static” factors such as depth to the CaCO₃ layer and SOC at the Canadian site, while
701 the R_m at large scales may be dominated by “dynamic” factors such as

702 meteorological anomaly. Compared to the SA model, estimation of spatially
703 distributed SWC was improved with the TA model at small watershed scales. This
704 was because the TA model considered a fair amount of spatial variance in
705 space variant temporal anomaly ~~the~~ R_m , which was ignored in the SA model.

Field Code Changed

Field Code Changed

Field Code Changed

706 Furthermore, the improved performance was observed mainly when there was less or
707 more soil water than was drier or wetter than the average level, especially in drier
708 conditions due to the high $\sigma_n^2(R_m)$ value.

709 ~~The TA model was combined with time stability analysis to estimate spatially~~
710 ~~distributed SWC and was compared with the SA model, where the SWC was~~
711 ~~decomposed into spatial mean SWC and spatial anomaly Z_m .~~

712 ~~The contributions of spatial variance of the R_m to the total variances of SWC~~
713 ~~were on average 118 and 19% in the near surface and the root zone, respectively.~~
714 ~~There were significant persistent spatial patterns (EOFs) of R_m over time, and the~~
715 ~~first pattern (EOF1) explained 61 and 44% of the total variance in the R_m for the~~
716 ~~near surface and root zone, respectively. Depth to the CaCO_3 layer and organic carbon~~
717 ~~content explained 81.6% (0–0.2 m) and 81.0% (0–1.0 m) of the variability in the~~
718 ~~EOF1 of R_m . Compared to the SA model, estimation of spatially distributed SWC~~
719 ~~was improved with the TA model. This was because the TA model considered a fair~~
720 ~~amount of spatial variance in space-variant temporal anomaly, which was ignored in~~
721 ~~the SA model. Furthermore, the improved performance was observed mainly when~~
722 ~~soil water was drier or wetter than the average level, especially in drier conditions due~~
723 ~~to the high $\sigma_n^2(R_m)$ value.~~ This study showed that outperformance of the TA model

724 over the SA model is possible when $\sigma_n^2(R_m)$ contributes substantial variance to the
725 total variances of SWC, and significant spatial patterns (or EOFs) exist in the R_m .

726 Further application of the TA model for the estimation of spatially distributed SWC at
727 different scales and hydrological backgrounds is recommended. If the TA model

728 parameters (i.e., M_{in} , EOF1 of the R_{in} , and relationship between EC and S_{in}) are
729 obtained from historical SWC datasets. This study also implies a potential in using the
730 TA model to construct a detailed spatially distributed SWC of near surface soil at
731 watershed scales can be constructed from remote sensed SWC. Note that both models
732 rely on previous SWC measurements for model parameters. Therefore, the future
733 study should be directed to estimate spatially distributed SWC in un-gauged
734 watersheds based on the estimation of the model parameters using pedotransfer
735 functions. Since the TA model needs one more spatial parameter (i.e., M_{in}) than the
736 SA model, the advantage of the TA model may be weakened. Nevertheless, the TA
737 model may be preferred if it estimates spatial SWC much better than the SA model
738 such as under dry conditions. The codes for decomposing SWC with the SA and TA
739 models and related EOF analysis were written in Matlab and are freely available from
740 the authors upon request.

Field Code Changed

Field Code Changed

Field Code Changed

Field Code Changed

741 **Acknowledgements**

742 This project was funded by the Natural Sciences and Engineering Research Council
743 (NSERC) of Canada. We thank Dr. Asim Biswas, Dr. Henry Wai Chau, Mr. Trent
744 Pernitsky, and Mr. Eric Neil for their help in data collection. We thank the anonymous
745 reviewers and the Editor for their constructive comments.

746 **References**

747 Biswas, A., Chau, H. W., Bedard-Haughn, A., and Si, B. C.: Factors controlling soil

748 water storage in the Hummocky landscape of the Prairie Pothole region of North
749 America, *Can. J. Soil Sci.*, 92, 649–663, doi: 10.4141/CJSS2011-045, 2012.

750 Biswas, A. and Si, B. C.: Scales and locations of time stability of soil water storage in
751 a hummocky landscape, *J. Hydrol.*, 408, 100–112, doi: 10.1016/j.jhydrol.2011.07.027,
752 2011.

753 Blöschl, G., Komma, J., and Hasenauer, S.: Hydrological downscaling of soil
754 moisture, Final report to the H-SAF (Hydrology Satellite Application Facility) via the
755 Austrian Central Institute for Meteorology and Geodynamics (ZAMG), Vienna
756 University of Technology, A-1040 Vienna, Austria, 2009.

757 Brocca, L., Melone, F., Moramarco, T., and Morbidelli, R.: Soil moisture temporal
758 stability over experimental areas in Central Italy, *Geoderma*, 148, 364–374, doi:
759 10.1016/j.geoderma.2008.11.004, 2009.

760 [Brocca, L., Tullo, T., Melone, F., Moramarco, T., and Morbidelli, R.: Catchment scale](#)
761 [soil moisture spatial-temporal variability, *J. Hydrol.*, 422-423, 63–75,](#)
762 [doi:10.1016/j.jhydrol.2011.12.039, 2012.](#)

763
764 Brocca, L., Zucco, G., Mittelbach, H., Moramarco, T., and Seneviratne, S. I.: Absolute
765 versus temporal anomaly and percent of saturation soil moisture spatial variability for
766 six networks worldwide, *Water Resour. Res.*, 50, 5560–5576, doi:
767 10.1002/2014WR015684, 2014.

768 [Brocca, L., Zucco, G., Moramarco, T., and Morbidelli, R.: Developing and testing a](#)
769 [long-term soil moisture dataset at the catchment scale, *J. Hydrol.*, 490, 144–151, doi:](#)

770 | [10.1016/j.jhydrol.2013.03.029](https://doi.org/10.1016/j.jhydrol.2013.03.029), 2013.

771 Burnham, K. P. and Anderson, D. R.: Model selection and multimodel inference: A
772 practical information-theoretic approach (2nd ed.), Springer-Verlag, New York, 2002.

773 Busch, F. A., Niemann, J. D., and Coleman, M.: Evaluation of an empirical
774 orthogonal function-based method to downscale soil moisture patterns based on
775 topographical attributes, *Hydrol. Process.*, 26, 2696–2709, doi: 10.1002/hyp.8363,
776 2012.

777 Champagne, C., Berg, A. A., McNairn, H., Drewitt, G., and Huffman, T.: Evaluation
778 of soil moisture extremes for agricultural productivity in the Canadian prairies, *Agric.
779 For. Meteorol.*, 165, 1–11, doi: 10.1016/j.agrformet.2012.06.003, 2012.

780 Famiglietti, J. S., Rudnicki, J. W., and Rodell, M.: Variability in surface moisture
781 content along a hillslope transect: Rattlesnake Hill, Texas, *J. Hydrol.*, 210, 259–281,
782 doi: 10.1016/S0022-1694(98)00187-5, 1998.

783 Gómez-Plaza, A., Alvarez-Rogel, J., Albaladejo, J., and Castillo, V. M.: Spatial
784 patterns and temporal stability of soil moisture across a range of scales in a semi-arid
785 environment, *Hydrol. Process.*, 14, 1261–1277, doi:
786 10.1002/(SICI)1099-1085(200005)14:7<1261::AID-HYP40>3.0.CO;2-D, 2000.

787 Gómez-Plaza, A., Martínez-Mena, M., Albaladejo, J., and Castillo, V. M.: Factors
788 regulating spatial distribution of soil water content in small semiarid catchments, *J.
789 Hydrol.*, 253, 211–226, doi: 10.1016/S0022-1694(01)00483-8, 2001.

790 Grant, L., Seyfried, M., and McNamara, J.: Spatial variation and temporal stability of
791 soil water in a snow-dominated, mountain catchment, *Hydrol. Process.*, 18,

792 3493–3511, doi: 10.1002/hyp.5789, 2004.

793 Grayson, R. B. and Western, A. W.: Towards areal estimation of soil water content
794 from point measurements: Time and space stability of mean response, *J. Hydrol.*, 207,
795 68–82, doi: 10.1016/S0022-1694(98)00096-1, 1998.

796 Hu, W., Shao, M. A., Han, F. P., and Reichardt, K.: Spatio-temporal variability
797 behavior of land surface soil water content in shrub- and grass-land, *Geoderma*, 162,
798 260–272, doi: 10.1016/j.geoderma.2011.02.008, 2011.

799 Hu, W., Shao, M. A., and Reichardt, K.: Using a new criterion to identify sites for
800 mean soil water storage evaluation, *Soil Sci. Soc. Am. J.*, 74, 762–773, doi:
801 10.2136/sssaj2009.0235, 2010.

802 Hu, W., Tallon, L. K., and Si, B. C.: Evaluation of time stability indices for soil water
803 storage upscaling, *J. Hydrol.*, 475, 229–241, doi: 10.1016/j.jhydrol.2012.09.050,
804 2012.

805 Jawson, S. D. and Niemann, J. D.: Spatial patterns from EOF analysis of soil moisture
806 at a large scale and their dependence on soil, land-use, and topographic properties,
807 *Adv. Water Resour.*, 30, 366–381, doi:10.1016/j.advwatres.2006.05.006, 2007.

808 Jia, Y. H. and Shao, M. A.: Temporal stability of soil water storage under four types of
809 revegetation on the northern Loess Plateau of China, *Agric. Water Manage.*, 117,
810 33–42, doi: 10.1016/j.agwat.2012.10.013, 2013.

811 Johnson, R. A. and Wichern, D. W.: *Applied multivariate statistical analysis*, Prentice
812 Hall, Upper Saddle River, New Jersey, 2002.

813 Joshi, C. and Mohanty, B. P.: Physical controls of near-surface soil moisture across

814 varying spatial scales in an agricultural landscape during SMEX02, *Water Resour.*
815 *Res.*, 46, doi: 10.1029/2010WR009152, 2010.

816 Korres, W., Koyama, C. N., Fiener, P., and Schneider, K.: Analysis of surface soil
817 moisture patterns in agricultural landscapes using Empirical Orthogonal Functions,
818 *Hydrol. Earth Syst. Sci.*, 14, 751–764, doi: 10.5194/hess-14-751-2010, 2010.

819 Martínez-Fernández, J. and Ceballos, A.: Temporal stability of soil moisture in a
820 large-field experiment in Spain, *Soil Sci. Soc. Am. J.*, 67, 1647–1656, 2003.

821 Millar, J. B.: Shoreline-area ratios as a factor in rate of water loss from small sloughs,
822 *J. Hydrol.*, 14, 259–284, doi: 10.1016/0022-1694(71)90038-2, 1971.

823 Mittelbach, H. and Seneviratne, I.: A new perspective on the spatio-temporal
824 variability of soil moisture: Temporal dynamics versus time-invariant contributions,
825 *Hydrol. Earth Syst. Sci.*, 16, 2169–2179, doi: 10.5194/hess-16-2169-2012, 2012.

826 Mohanty, B. P. and Skaggs, T. H.: Spatio-temporal evolution and time-stable
827 characteristics of soil moisture within remote sensing footprints with varying soil
828 slope and vegetation, *Adv. Water Resour.*, 24, 1051–1067, doi:
829 10.1016/S0309-1708(01)00034-3, 2001.

830 Peel, M. C., Finlayson, B. L., and McMahon, T. A.: Updated world map of the
831 Köppen-Geiger climate classification, *Hydrol. Earth Syst. Sci.*, 11, 1633–1644,
832 doi:10.5194/hess-11-1633-2007, 2007.

833 Perry, M. A. and Niemann J. D.: Analysis and estimation of soil moisture at the
834 catchment scale using EOFs, *J. Hydrol.*, 334, 388–404, doi:
835 10.1016/j.jhydrol.2006.10.014, 2007.

836 Perry, M. A. and Niemann J. D.: Generation of soil moisture patterns at the catchment
837 scale by EOF interpolation, *Hydrol. Earth Syst. Sci.*, 12, 39–53,
838 doi:10.5194/hess-12-39-2008, 2008.

839 Robinson, D. A., Campbell, C. S., Hopmans, J. W., Hornbuckle, B. K., Jones, S. B.,
840 Knight, R., Ogden, F., Selker, J., and Wendroth, O.: Soil moisture measurement for
841 ecological and hydrological watershed-scale observatories: A review, *Vadose Zone J.*,
842 7, 358–389, doi: 10.2136/vzj2007.0143, 2008.

843 Rötzer, K., Montzka, C., and Vereecken, H.: Spatio-temporal variability of global soil
844 moisture products, *J. Hydrol.*, 522, 187–202, doi: 10.1016/j.jhydrol.2014.12.038,
845 2015.

846 She, D. L., Liu, D. D., Peng, S. Z., and Shao, M. A.: Multiscale influences of soil
847 properties on soil water content distribution in a watershed on the Chinese Loess
848 Plateau, *Soil Sci.*, 178, 530–539, doi: 10.1016/j.jhydrol.2014.08.034, 2013a.

849 She, D. L., Xia, Y. Q., Shao, M. A., Peng, S. Z., and Yu, S. E.: Transpiration and
850 canopy conductance of *Caragana Korshinskii* trees in response to soil moisture in
851 sand land of China, *Agrofor. Syst.*, 87, 667–678, doi: 10.1007/s10457-012-9587-4,
852 2013b.

853 Sherratt, D. J. and Wheeler, H. S.: The use of surface-resistance soil-moisture
854 relationships in soil-water budget models, *Agric. For. Meteorol.*, 31, 143–157, doi:
855 10.1016/0168-1923(84)90016-9, 1984.

856 Soil Survey Staff: *Soil Taxonomy*, 11th edition, USDA National Resources
857 Conservation Services, Washington DC, 2010.

858 Starr, G. C.: Assessing temporal stability and spatial variability of soil water patterns
859 with implications for precision water management, *Agric. Water Manage.*, 72,
860 223–243, doi: 10.1016/j.agwat.2004.09.020, 2005.

861 Vachaud, G., De Silans, A. P., Balabanis, P., and Vauclin, M.: Temporal stability of
862 spatially measured soil water probability density function, *Soil Sci. Soc. Am. J.*, 49,
863 822–828, 1985.

864 van der Kamp, G., Hayashi, M., and Gallen, D.: Comparing the hydrology of grassed
865 and cultivated catchments in the semi-arid Canadian prairies, *Hydrol. Process.*, 17,
866 559–575, doi: 10.1002/hyp.1157, 2003.

867 Vanderlinden, K., Vereecken, H., Hardelauf, H., Herbst, M., Martinez, G., Cosh, M.
868 H., and Pachepsky, Y. A.: Temporal stability of soil water contents: A review of data
869 and analyses, *Vadose Zone J.*, 11, 4, doi: 10.2136/vzj2011.0178, 2012.

870 Vereecken, H., Kamai, T., Harter, T., Kasteel, R., Hopmans, J., and Vanderborght, J.:
871 Explaining soil moisture variability as a function of mean soil moisture: A stochastic
872 unsaturated flow perspective, *Geophys. Res. Lett.*, 34, L22402, doi:
873 10.1029/2007GL031813, 2007.

874 Venkatesh, B., Nandagiri, L., Purandara, B. K., and Reddy, V. B.: Modelling soil
875 moisture under different land covers in a sub-humid environment of Western Ghats,
876 India, *J. Earth Syst. Sci.*, 120, 387–398, 2011.

877 Walsh, J. E. and Mostek, A.: A quantitative-analysis of meteorological anomaly
878 patterns over the United-States, 1900–1977, *Mon. Weather Rev.*, 108, 615–630, doi:
879 10.1175/1520-0493(1980)108<0615:AQAOMA>2.0.CO;2, 1980.

880 Wang, Y. Q., Shao, M. A., Liu, Z. P., and Warrington, D. N.: Regional spatial pattern
881 of deep soil water content and its influencing factors, *Hydrolog. Sci. J.*, 57, 265–281,
882 doi: 10.1080/02626667.2011.644243, 2012.

883 Ward, P. R., Flower, K. C., Cordingley, N., Weeks, C., and Micin, S. F.: Soil water
884 balance with cover crops and conservation agriculture in a Mediterranean climate,
885 *Field Crop. Res.*, 132, 33–39, doi: 10.1016/j.fcr.2011.10.017, 2012.

886 Zhao, Y., Peth, S., Wang, X. Y., Lin, H., and Horn, R.: Controls of surface soil
887 moisture spatial patterns and their temporal stability in a semi-arid steppe, *Hydrol.*
888 *Process.*, 24, 2507–2519, doi: 10.1002/hyp.7665, 2010.

889 **Figure captions**

890 **Figure 1.** Decomposition of spatiotemporal soil water content (SWC) in different
891 models.

892 **Figure 2.** Daily mean air temperature and precipitation during the study period.

893 **Figure 23.** Components of soil water content in (a) the SA model: ~~(a)~~ (spatial mean
894 soil water content S_{in} and ~~(b)~~ spatial anomaly Z_m ~~on a dry day (23 August 2008)~~
895 ~~and a wet day (13 May 2011)~~ and in (b) the TA model (time-stable pattern M_{in} , ~~(b)~~
896 space-invariant temporal anomaly A_{in} , and ~~(c)~~ space-variant temporal anomaly R_m)
897 for 0–0.2 and 0–1.0 m. Also shown is the ~~relative~~ elevation.

898 **Figure 34.** (a) The EOF1 of the spatial anomaly Z_m and (b) relationships of
899 associated EC1 versus spatial mean soil water content Z_m fitted by the cosine
900 function (Eq.4).

901 ~~**Figure 4.** Components of soil water content of the TA model: (a) time stable pattern~~
902 ~~M_{in} , (b) space-invariant temporal anomaly A_{in} , and (c) space-variant temporal~~
903 ~~anomaly R_m on a dry day (23 August 2008) and a wet day (13 May 2011) for 0–0.2~~
904 ~~and 0–1.0 m. Also shown are relative elevation, daily mean air temperature, and daily~~
905 ~~precipitation.~~

906 **Figure 5.** Spatial variances of different components in Eq. (8) expressed in %² (upper
907 panel) and as percentage (lower panel) for (a) 0–0.2 and (b) 0–1.0 m. Spatial mean
908 soil water content S_{in} on each measurement day is also shown.

909 **Figure 6.** (a) The EOF1 of the space-variant temporal anomaly R_m and (b)
910 relationships of associated EC1 versus spatial mean soil water content S_{in} fitted by

911 the cosine function (Eq. 4).

912 **Figure 7.** Estimated soil water content (SWC) versus measured SWC for three dates
913 at different soil water conditions (~~23~~-August 23, 2008, ~~27~~-October 27, 2009, and ~~13~~
914 May 13, 2011 are associated with relatively dry, medium, and wet days, respectively)
915 using the TA model for (a) 0–0.2 ~~m~~ and (b) 0–1.0 m.

916 **Figure 8.** The Nash-Sutcliffe coefficient of efficiency (NSCE) of soil water content
917 estimation using the TA and SA models ~~at~~-for (a) 0–0.2 ~~m~~ and (b) 0–1.0 m for both
918 cross validation (CV) and external validation (EV). At 0–0.2 m, negative
919 Nash-Sutcliffe coefficient of efficiency values for three dates (~~22~~-October 22, 2008,
920 ~~27~~-August 27, 2009, and ~~27~~-October 27, -2009) are not shown. Spatial mean soil
921 water content S_{in} on each measurement day is also shown.

922 **Figure 9.** Difference between the Nash-Sutcliffe coefficient of efficiency (NSCE) of
923 soil water content ~~evaluation estimation by both cross validation (CV) and external~~
924 validation (EV) using the TA and ~~the~~-SA models as a function of space-invariant
925 temporal anomaly A_{in} ~~at~~-for (a) 0–0.2 ~~m~~ and (b) 0–1.0 m.

926
927 **Figure 10.** Difference between the Nash-Sutcliffe coefficient of efficiency (NSCE) of
928 soil water content evaluation by the cross validation using the TA and SA models as a
929 function of space-invariant temporal anomaly A_{in} for (a) 0–0.06 m of the Chinese
930 Loess Plateau hillslope and (b) 0–0.15 m of the GENCAI network in Italy.

Formatted: Line spacing: Double

Field Code Changed

Table 1. Pearson correlation coefficients between time-stable pattern $M_{\hat{m}}$, EOF1 of space-variant temporal anomaly R_{m} and various properties.

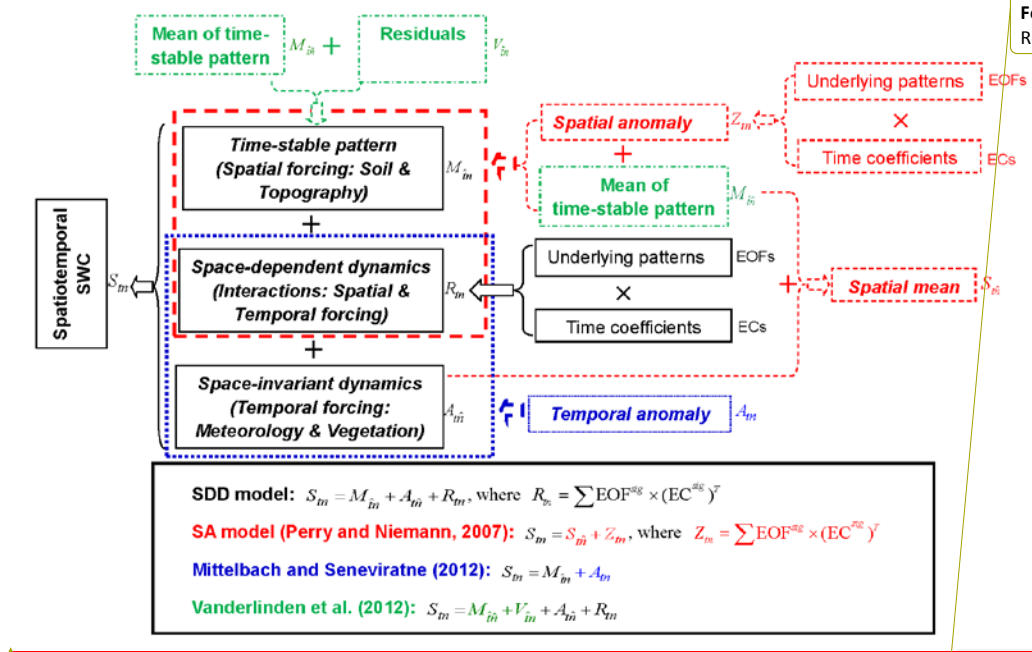
	0–0.2 m		0–1.0 m	
	$M_{\hat{m}}$	EOF1	$M_{\hat{m}}$	EOF1
Sand content	-0.52**	-0.36**	-0.66**	-0.26**
Silt content	0.29**	0.14	0.40**	0.06
Clay content	0.43**	0.38**	0.51**	0.33**
Organic carbon	0.78**	0.83**	0.73**	0.76**
Wetness index	0.64**	0.59**	0.68**	0.56**
Depth to CaCO ₃ layer	0.77**	0.84**	0.65**	0.88**
A horizon depth	0.51**	0.62**	0.44**	0.65**
C horizon depth	0.66**	0.69**	0.58**	0.76**
Bulk density	-0.58**	-0.67**	-0.46**	-0.62**
Elevation	-0.24**	-0.28**	-0.24**	-0.32**
Specific contributing area	0.20*	0.24**	0.24**	0.23**
Convergence index	-0.58**	-0.56**	-0.55**	-0.58**
Curvature	-0.10	-0.08	-0.19*	-0.16
Cos(aspect)	0.05	0.04	0.08	0.05
Gradient	-0.12	-0.09	-0.21*	-0.02
Slope	-0.51**	-0.48**	-0.56**	-0.44**
Upslope length	0.19*	0.21*	0.21*	0.25**
Solar radiation	-0.07	0.03	-0.11	0.08
Flow connectivity	0.45**	0.43**	0.49**	0.49**
Leaf area index	-0.07	0.06	-0.10	-0.14
Variance explained ¹	74.5%	81.6%	75.6%	81.0%

¹percent of variance explained by the controlling factors obtained by the multiple stepwise regressions.

*Significant at $P<0.05$; ** Significant at $P<0.01$.

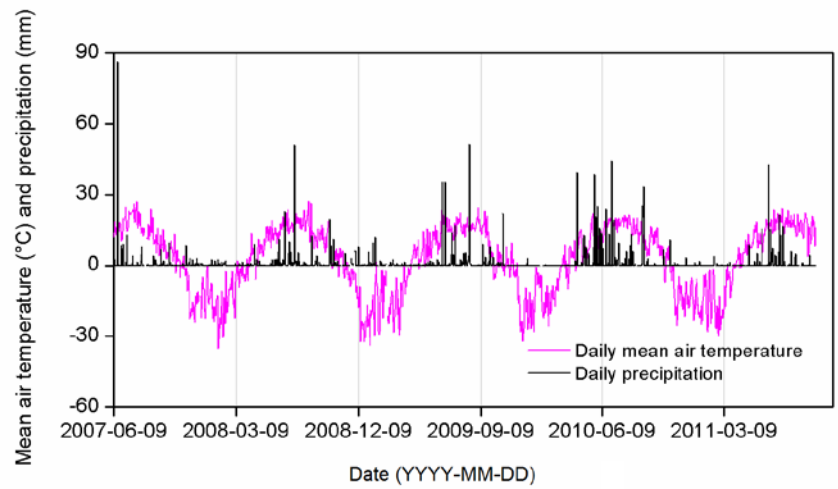
Table A1. Notations.

$M_{\hat{m}}$	spatial mean of $M_{\hat{m}}$
R_m	space-variant temporal anomaly of SWC at location n and time t
$A_{\hat{m}}$	space-invariant temporal anomaly of SWC at time t
Z_m	spatial anomaly of SWC at location n and time t
$S_{\hat{m}}$	spatial mean SWC at time t
$\sigma_{\hat{m}}^2$	spatial variance
A_m	temporal anomaly of SWC at location n and time t
$\delta_{\hat{m}}$	temporal mean relative difference of SWC at location n
COV	spatial covariance
S_m	SWC at location n and time t
$M_{\hat{m}}$	time-stable pattern of SWC
ECs	temporally-varying coefficients of R_m (or Z_m)
EOFs	time-invariant spatial structures of R_m (or Z_m)
NSCE	Nash-Sutcliffe coefficient of efficiency
R	Pearson correlation coefficient
SWC	soil water content



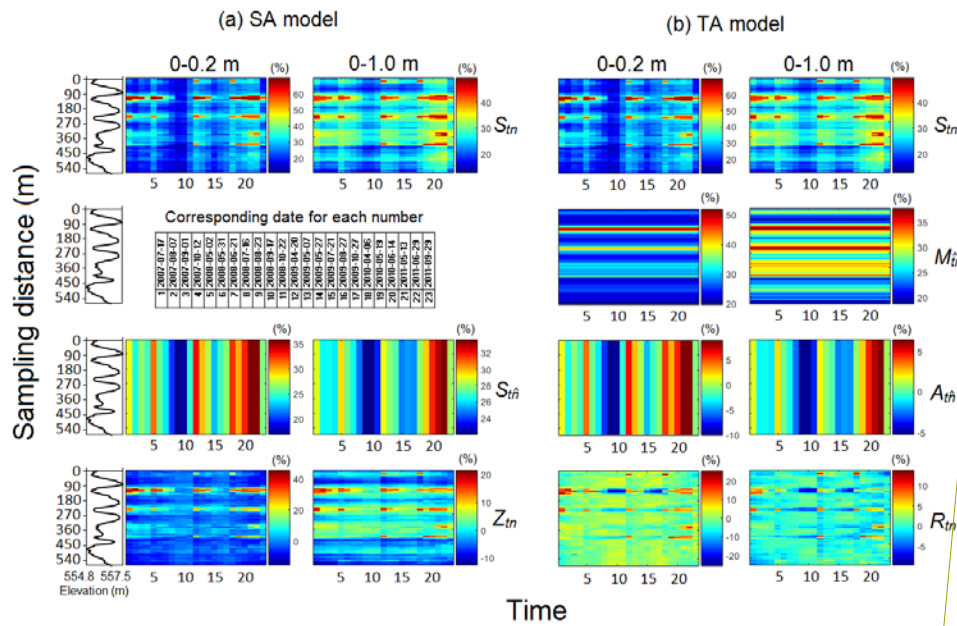
Formatted: Font: (Default) Times New Roman, 12 pt, Font color: Text 1

Fig. 1. Decomposition of spatiotemporal soil water content (SWC) in different models.



Formatted: Font: (Default) Times New Roman, 12 pt, Font color: Text 1

Fig. 2. Daily mean air temperature and precipitation during the study period.



Formatted: Font: (Default) Times New Roman, 12 pt, Font color: Text 1

Fig. 3. Components of soil water content in (a) the SA model (spatial mean soil water content S_m and spatial anomaly Z_m) and in (b) the TA model (time-stable pattern M_m , space-invariant temporal anomaly A_m , and space-variant temporal anomaly R_m) for 0–0.2 and 0–1.0 m. Also shown is the elevation.

Field Code Changed

Field Code Changed

Field Code Changed

Field Code Changed

Field Code Changed

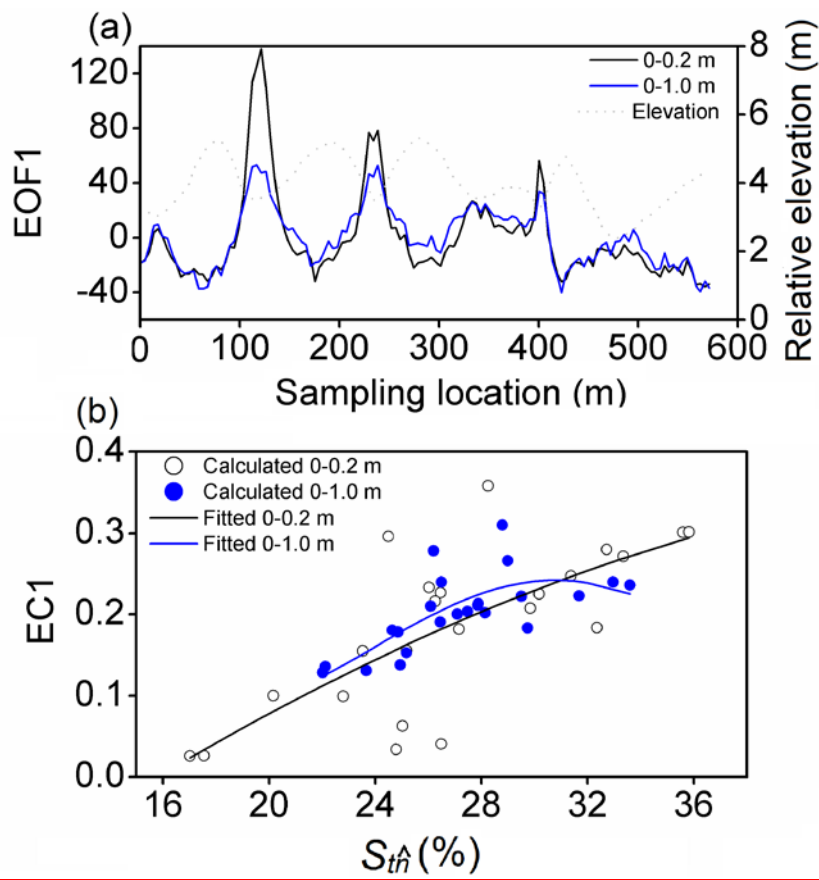


Fig. 4. (a) The EOF1 of the spatial anomaly Z_m and (b) relationships of associated EC1 versus spatial mean soil water content $S_m^{\hat{}}$ fitted by the cosine function (Eq. 4).

Formatted: Font: (Default) Times New Roman, 12 pt, Font color: Text 1

Field Code Changed

Field Code Changed

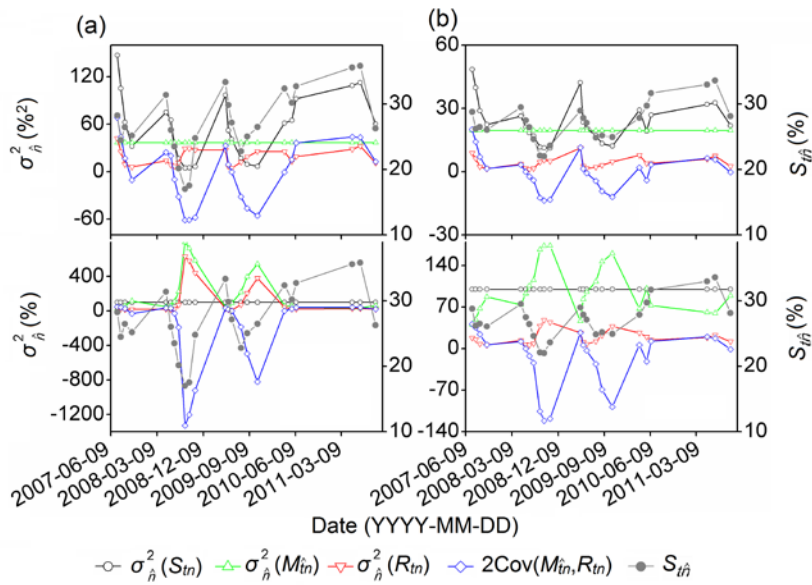


Fig. 5. Spatial variances of different components in Eq. (8) expressed in %² (upper panel) and as percentage (lower panel) for (a) 0–0.2 and (b) 0–1.0 m. Spatial mean soil water content S_{in} on each measurement day is also shown.

Formatted: Font: (Default) Times New Roman, 12 pt, Font color: Text 1

Field Code Changed

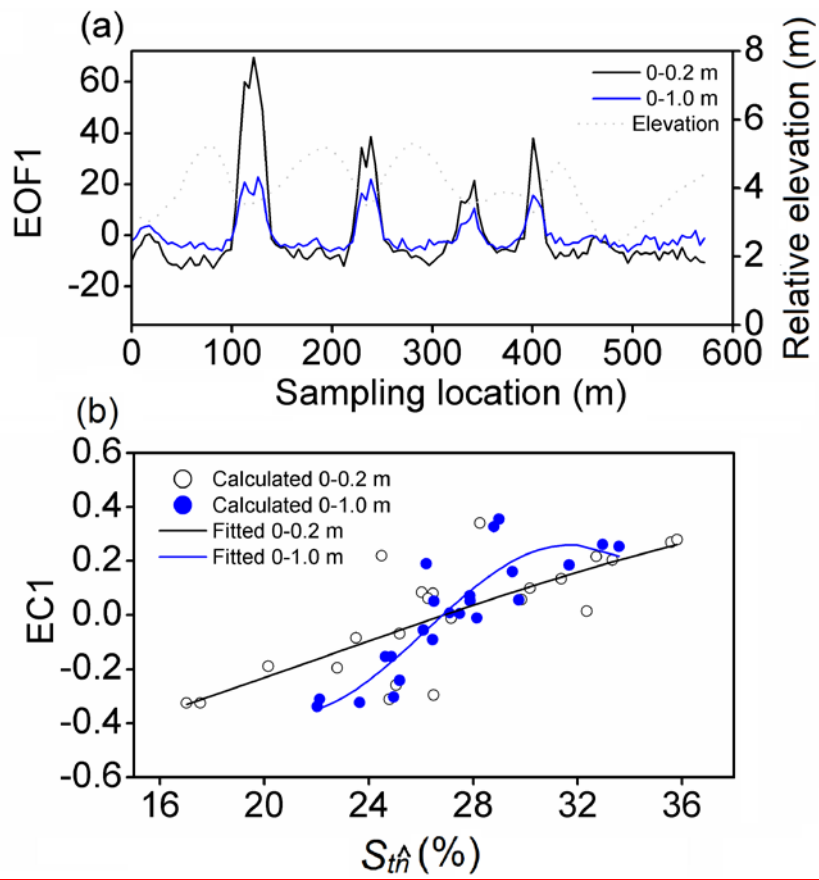
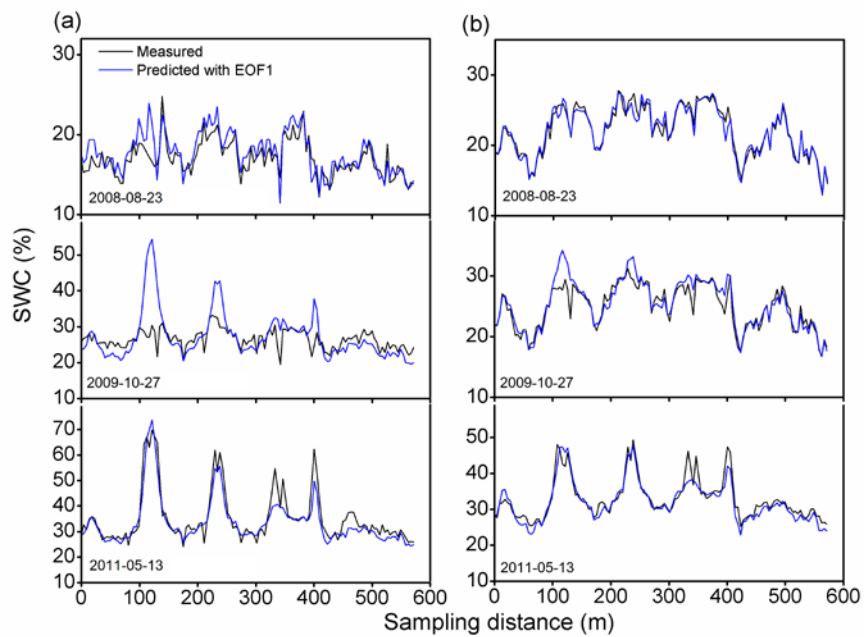


Fig. 6. (a) The EOF1 of the space-variant temporal anomaly R_m and (b) relationships of associated EC1 versus spatial mean soil water content $S_{\hat{t}n}$ fitted by the cosine function (Eq. 4).

Formatted: Font: (Default) Times New Roman, 12 pt, Font color: Text 1

Field Code Changed

Field Code Changed



Formatted: Font: (Default) Times New Roman, 12 pt, Font color: Text 1

Fig. 7. Estimated soil water content (SWC) versus measured SWC for three dates at different soil water conditions (August 23, 2008, October 27, 2009, and May 13, 2011 are associated with relatively dry, medium, and wet days, respectively) using the TA model for (a) 0–0.2 and (b) 0–1.0 m.

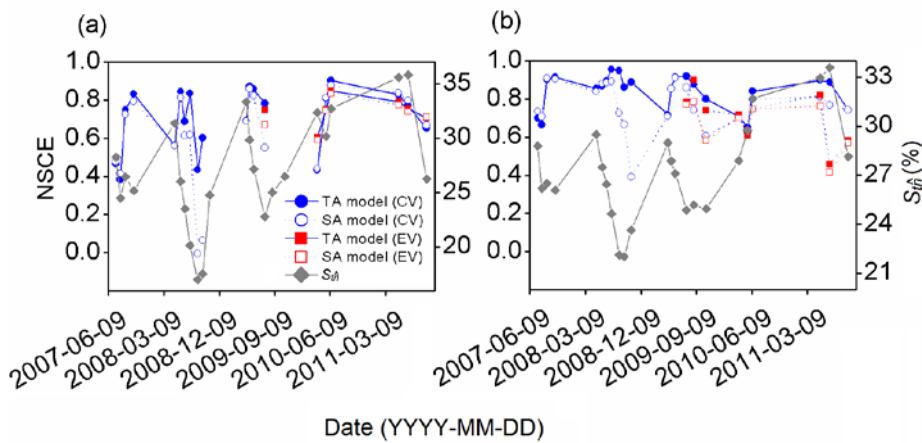


Fig. 8. The Nash-Sutcliffe coefficient of efficiency (NSCE) of soil water content estimation using the TA and SA models for (a) 0–0.2 and (b) 0–1.0 m for both cross validation (CV) and external validation (EV). At 0–0.2 m, negative Nash-Sutcliffe coefficient of efficiency values for three dates (October 22, 2008, August 27, 2009, and October 27, 2009) are not shown. Spatial mean soil water content S_m on each measurement day is also shown.

Formatted: Font: (Default) Times New Roman, 12 pt, Font color: Text 1

Field Code Changed

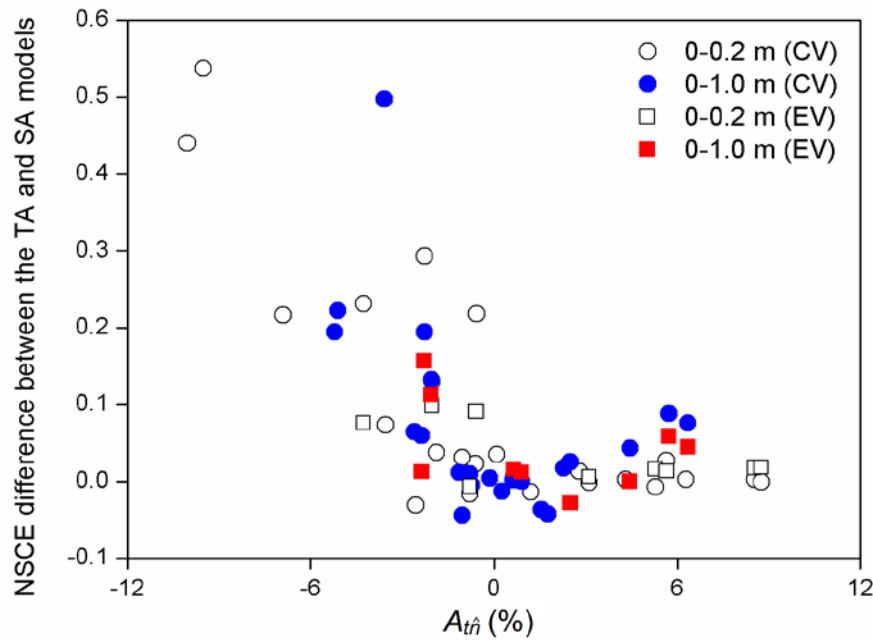


Fig. 9. Difference between the Nash-Sutcliffe coefficient of efficiency (NSCE) of soil water content estimation by both cross validation (CV) and external validation (EV) using the TA and SA models as a function of space-invariant temporal anomaly $A_{t\hat{m}}$ for (a) 0–0.2 and (b) 0–1.0 m.

Formatted: Font: (Default) Times New Roman, 12 pt, Font color: Text 1

Field Code Changed

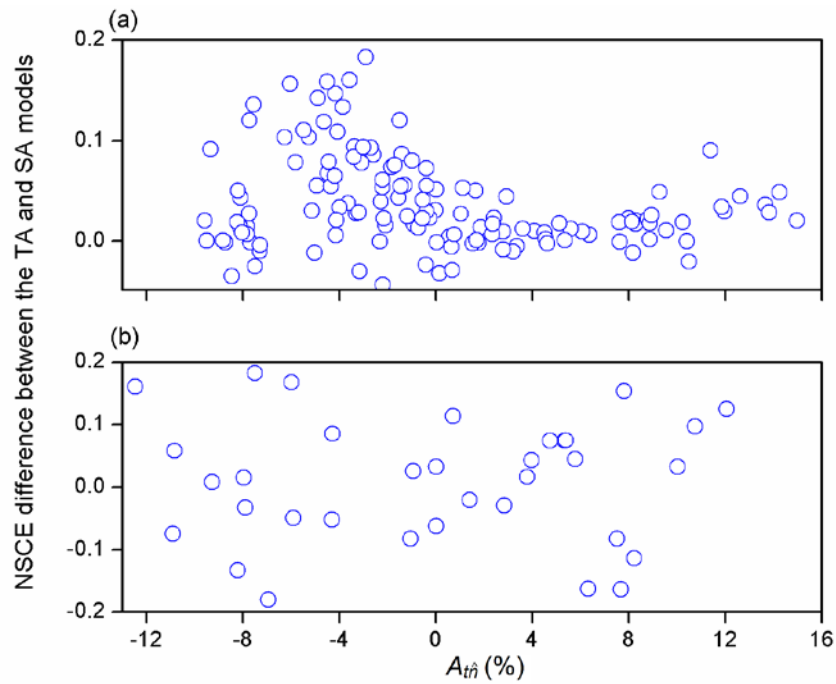


Fig. 10. Difference between the Nash-Sutcliffe coefficient of efficiency (NSCE) of soil water content evaluation by the cross validation using the TA and SA models as a function of space-invariant temporal anomaly A_{tn} for (a) 0–0.06 m of the Chinese Loess Plateau hillslope and (b) 0–0.15 m of the GENCAI network in Italy.

Formatted: Font: (Default) Times New Roman, 12 pt, Font color: Text 1

Field Code Changed